Donders Graduate School for Cognitive Neuroscience
Master of Science Programme
MSc Thesis

Fear to approach; identifying behavioural and neurological mechanisms underlying excessive avoidance behaviour.

by

Anna Wester

Supervised by:

1. Dr. Floris Klumpers
2. Anneloes Hulsman
3. Prof. Dr. Erno Hermans

Radboud University Nijmegen

Date of final oral examination: 29-08-2022

Abstract

Excessive avoidance has been marked as a transdiagnostic symptom involved in both depressive and anxiety disorders. Recent findings have indicated that these avoidance behaviours are a better indication of poor prognosis than other measures. Real-life approach-avoidance decisions rely on a complex consideration of potential rewarding and potential threatening consequences. However, preceding research on approach-avoidance decisions is often centred around the threat component of the decision-making. To obtain a deeper understanding of the shared mechanisms that are underlying depressive and anxiety disorders, we assessed the behavioural and neurological correlates of avoidance behaviours in a two-study research project. For this purpose, we used two different, yet similar, approach-avoidance decision-making paradigms, being the fearful avoidance task (FAT) and the passive-active approach-avoidance task (PAT). Both paradigms effectively evoked an approach-avoidance conflict due to the inclusion of competing threat and reward levels. Using whole-brain searchlight Multi-Variate Pattern Analysis (MVPA), we identified an approach-avoidance decision-making network consisting of the precuneus, postcentral gyrus, precentral gyrus, medial prefrontal cortex, and medial orbitofrontal cortex (study 1, N = 27). Additionally, focussing on the reward components of complex decision-making, we assessed whether anhedonia, a symptom characterized by attenuated reward sensitivity, could explain individual differences in approach-avoidance decision-making (study 2, N = 15). Considering the small sample size, we identified that higher anhedonia is paired with more avoidance (non-significant). Taken all together, we have showed that approach-avoidance decision-making relies on a complex cognitive consideration of potential threat and reward, implicating a network of various brain regions related to emotional experience, decision-making, motor preparation, goal-directed behaviour, and reward and threat assessment.

Keywords: MVPA, Avoidance, Decision Making, Anhedonia, Anxiety, Depression

Introduction

Anxiety and depressive disorders are two of the most prevalent mental disorders worldwide, occurring in people of all ages (Kessler, Petukhova, Sampson, Zaslavsky & Wittchen, 2012; de Graaf et al., 2013; Khalid, Qadir, Chan & Schwannauer, 2019; Auerbach et al., 2016). These two disorders are both ranked within the top 25 of leading causes of the global health-related burden (Santomauro et al., 2021). On top of this, the COVID-19 pandemic caused for a further increase in prevalence of these disorders. Therefore, there is an increasing urgency to invest in research focusing on understanding the behavioural and neural mechanisms that are driving these psychopathologies, to be able to come up with novel treatment solutions.

To find such novel treatment targets, it is important to look beyond the clinical diagnoses and investigate potential transdiagnostic behavioural and neurological mechanisms. An example of an initiative that advocates toward such an approach can be found in the RDoC Research Domain Criteria (Cuthbert & Insel, 2013). The reason why we have to look for targets that are shared between psychopathologies, is because current treatments prescribed based on a clinical diagnosis are often ineffective, resulting in high relapse rates. As an example, relapse rates were 40 percent when depressed patients underwent psychotherapy, and remained 23 percent when treated with an additional antidepressant (Steinert, Hofmann, Kruse & Leichsenring, 2014; Williams, Simpson, Simpson & Nahas, 2009). Anxiety patients that are treated with psychotherapy and SSRI's also relapsed in 16.4 percent of the cases (Batelaan et al., 2017). In addition to high prevalence and relapse rates, these disorders are often comorbid. A study in the Netherlands has for instance indicated that 67 percent of all people with a clinical depression also suffer from anxiety, and that 63 percent of the anxiety patients have a comorbid depressive disorder (Lamers et al., 2011). This indicates that these psychopathologies might partially share aetiology. With the current research, we aim to add to the understanding of anxiety and depressive disorders, by investigating the neural and behavioural mechanisms of excessive avoidance.

Excessive avoidance behaviour has been notified to be of importance in both the onset and maintenance of anxiety- and depressive disorders and could hence potentially function as a transdiagnostic construct underlying these psychopathologies (Cremers, Veer, Spinhoven, Rombouts & Roelofs, 2015; Trew, 2011; Carvalho & Hopko, 2011). That is, research has shown that avoidance hinders anxious individuals in taking part in social interactions, leading to an abstinence of positive reinforcement, which in turn maintains the avoidance behaviours (Cremers, Veer, Spinhoven, Rombouts & Roelofs, 2015). In addition to social situations, anxious individuals can show excessive fear, anxiety, and avoidance towards other unfamiliar situations, or with themselves (Pittig, Treanor, LeBeau & Craske, 2018). Additionally, anxious individuals lack the motivational preference for (social) rewards (Cremers, Veer, Spinhoven, Rombouts & Roelofs, 2015). These findings suggest that anxious patients might suffer from a disrupted motivational system, leading to less approach behaviour, less positive reinforcement, and elevated anxiety symptoms. In depressed individuals, excessive avoidance leads to passivity and withdrawal, causing for limited access to sources of positive reinforcement as well, which promotes a negative information processing bias (Trew, 2011; Carvalho & Hopko, 2011). This can in turn sustain or worsen depressive symptoms and is therefore relevant to both the onset and the maintenance of depression (Carvalho & Hopko, 2011). Additionally, research has showed that increased

avoidance might be a better predictor of poor prognosis than other measures (Hendriks et al., 2012 Pittig, Alpers, Niles, & Craske , 2015). Based on these findings, it is of interest to investigate what neural and behavioural response patterns can explain such excessive avoidance.

Approach or avoidance decisions are often the result of a conflict between perceived potential reward and perceived potential threat (Pittig & Scherbaum, 2020; Bublatzky, Alpers & Pittig, 2017). However, this interaction or balance between different levels of reward and threat in approach-avoidance decision-making remains understudied. That is, previous studies have often not investigated the effects of reward in avoidance decisions. Additionally, behavioural avoidance paradigms commonly consist of just one positive and/or negative outcome, leading to an increase in decisions that lead to a positive outcome, and a decrease in behaviours that lead to a negative outcome (Richards, Plate & Ernst, 2013; Pittig, Treanor, LeBeau & Craske, 2018). Real-life approach-avoidance decision-making, however, relies on a more complex interplay of potential rewarding and threatening consequences that are competing against one another (Krypotos, Vervliet & Engelhard, 2018; Pittig, Treanor, LeBeau & Craske, 2018). In our study, we therefore assessed the mechanisms that are driving these advanced decisions in more complex, ambiguous paradigms, that included both rewarding and threatening components.

Previous research focusing on approach-avoidance decision-making that included this complex interaction between reward and threat components, has demonstrated that reward and threat have opposing effects on the proportion of avoidance decisions (Hulsman et al., 2021). In a magnetic resonance imaging (MRI) study, the same authors showed that increased activation in reward- and threat related brain regions such as the dorsal anterior cingulate cortex (dACC), amygdala and bed nucleus stria terminalis (BNST) was related to increasing levels of reward (Hulsman et al., in prep.). They furthermore indicated that the decision to avoid a certain combination of reward and threat was associated with decreased nucleus accumbens (NAcc) activity. Previous research in humans and macaque monkeys indicated the anterior cingulate cortex (ACC) as the hub for approach-avoidance conflict (Ironside et al., 2020; Livermore, et al., 2021). Although the role of the ACC in approach-avoidance decision-making seems relatively prominent across different studies, there are numerous other brain regions that have been associated with approach-avoidance decisions. Different research paradigms mention the importance of salience network brain regions such as the anterior insula, thalamus and dACC, threat-related regions as the amygdala and bed nucleus stria terminalis (BNST) or reward-related regions such as the NAcc, dorsomedial prefrontal cortex (dmPFC) and striatum, while at the same time stressing the importance of higher-order integrative brain regions such as the ventral striatum, dorsolateral prefrontal cortex (dlPFC), ventromedial prefrontal cortex (vmPFC) and lateral prefrontal cortex (lPFC) in making these decisions (McDermott et al., 2021; Schlund & Dymond, 2016; Zorowitz et al., 2019; Aupperle, Melrose, Francisco, Paulus & Stein, 2014; Spielberg et al., 2012, O'Neil et al., 2015; Talmi, Dayan, Kiebel, Frith & Dolan, 2009; Basten, Biele, Heekeren & Fiebach, 2010).

As reward components are commonly overlooked in avoidance paradigms, it is possible that the variance seen in avoidance decision-making could be explained by anhedonia. Anhedonia, a clinical symptom of depressive disorders (American Psychiatric Association, 2013), has been defined as a state characterized by a diminished capacity to experience

pleasure (Pelizza & Ferrari, 2009). This is commonly reflected in a lack of interest in – and withdrawal from – activities that were previously regarded pleasantly. It has been shown that anhedonia is caused by an inability to process positive reinforcement and by attenuated reward sensitivity, which in turn can lead to the onset of depression (Alloy, Olino, Freed & Nusslock, 2016; Liu et al., 2016). Besides being one of the core features of depressive disorders, it has been shown that characteristics of anhedonia are also found in many other disorders and diseases (Dillon et al., 2013; Sharma et al., 2017; Zhang et al., 2015). Taylor, Hoffman and Khan (2022) have even suggested that anhedonia hinders key processes that are involved in resolving anxiety disorders. Given that a lacking drive towards positive reinforcement could lead to a bias towards avoidance behaviours, we investigated whether excessive avoidance can be further explained by anhedonia symptoms, to deepen our understanding of the mechanisms that drive psychopathology.

In study 1 of this research project, we used Multi-Voxel Pattern Analysis (MVPA), to investigate which brain regions are incorporated in a network that is responsible for approach-avoidance decision-making. This influential functional MRI (fMRI) data analysis technique allows for a model-free pattern analysis using machine learning techniques (Mahmoudi, Takerkart, Regragui, Boussaoud & Brovelli, 2012). A classifier searches for highly reproducible spatial patterns of activity that differentiate across experimental conditions, and thereby captures the relationship between the fMRI activity across the brain, and an experimental condition. Using this method allowed us to shed light on which brain regions are implicated in the decision to approach or to avoid.

Specifically, with our first study, we aimed at investigating what brain network is involved in deciding to approach or avoid a certain combination of reward and threat. As said, approach-avoidance decision-making is often the result of an internal conflict between perceived reward and threat. Based on previous research, we therefore expected to find a network including several reward-related brain regions such as the NAcc (Hulsman et al., in prep.), as well as threat-associated regions as the amygdala (Hulsman et al., in prep.; Spielberg et al., 2012; Basten, Biele, Heekeren, & Fiebach, 2010), and regions that are commonly related to decision-making, such as the dmPFC and ACC (Schlund & Dymond, 2016; Aupperle, Melrose, Francisco, Paulus & Stein, 2014; Talmi, Dayan, Kiebel, Frith & Dolan, 2009; Basten, Biele, Heekeren & Fiebach, 2010). With this, we aimed to deepen our understanding of the mechanisms that underlie approach-avoidance decision-making and tried to find a multifaceted network of activity that represented complex approach-avoidance decisions in the presence of both potential rewards and potential threats.

As stated before, the second aim of the current research project was to investigate whether excessive avoidance could be further explained by anhedonia. To this end, we conducted a second study using a similar approach-avoidance decision-making paradigm. We investigated whether the total score on the Dimensional Anhedonia Rating Scale (DARS) could explain unique variance in approach and avoidance. As we also tried to conceptually replicate the results from Hulsman et al. (in prep.) with a different task design, we compared the results regarding the approach-avoidance decisions to the outcomes of this previous study, to see if we would find similar results using our novel task design.

Experiment 1
Methods

Participants

In this study, 31 healthy participants were recruited (male = 14, female = 17) to participate in the experiment. All participants met the a priori pre-registered inclusion criteria regarding the number of missing responses, adequateness of the response patterns and quality of the fMRI data (for details, see the preregistration of Hulsman, Klaassen, Roelofs & Klumpers, 2021: https://osf.io/7sm9k). As the between-run approach-avoidance classification requires both approach and avoidance responses within each block to be able to make comparable neural estimates for the two different response types, we had to include an additional exclusion criterion for the specific purpose of this study. That is, participants had to be excluded from the MVPA analyses if they lacked approach or avoidance responses in at least one of the five trial blocks. This resulted in the exclusion of four participants, creating a total sample size of 27 participants (male = 13, female = 14). The mean age of the participants was 23.3 (SD = 3.4, range = 19-33 years).

All participants received a fixed monetary compensation for their participation in the study. In addition, participants could earn a bonus depending on how they performed in the task. The study was approved by the local ethical committee (CMO Arnhem-Nijmegen) and was executed in compliance with these guidelines.

Fearful Avoidance Task (FAT)

Before starting the fearful avoidance task (FAT), participants underwent a standardized shock-work-up procedure (described in Klumpers et al., 2010), consisting of 5 electrical stimulations to titrate the shock intensities to an uncomfortable, yet not painful level. Additionally, participants performed a monetary titration task that consisted of monetary rewards ranging from €0.20 to €10.00. During the titration task, participants were consecutively presented with one of the monetary values in a counterbalanced manner and were requested to choose between two options that would lead to different hypothetical outcomes. The first option would hypothetically lead to receiving a positive outcome (the monetary reward) in 40 percent of the cases, to receiving a negative outcome (electrical stimulations) in 40 percent of the cases, and to receiving a neutral outcome (no stimulations nor monetary reward) in 20 percent of the cases. The other option hypothetically resulted in a positive outcome with 10 percent chance, a negative outcome with 10 percent chance, and a neutral outcome in 80 percent of the cases. Using this titration task, we could determine a monetary tipping point that was subsequently used in the FAT, to ensure that participants subjectively experienced similar reward-threat trade-offs. Low reward levels in the FAT were monetary rewards between 40 and 50 percent below the individual tipping point, medium reward levels between -5 and 5 percent below and above the tipping point, and high monetary reward levels varied between 40 and 50 percent above the tipping point.

Instructions of the FAT were presented on a computer screen. The procedure of the FAT is displayed in figure 1B. Participants were informed that different avatars would appear throughout the task and were told which threat level belonged to which avatar (see figure 1A for an example). The indicated threat level corresponded to the duration of the electrical stimulation (being 5, 35 or 250 ms) that the participants could potentially receive. During the

offer and decision phase, one of the avatars would appear on the screen for a duration of 2.5 seconds. Additionally, to establish the reward-threat trade-off, the reward level of the trial was indicated by the amount of money that could be won with this trial, belonging to the low, medium, or high monetary rewards. The amount of money was displayed in text below the avatar. All combinations between reward and threat were created in a full-factorial manner, resulting in nine reward-threat combinations. All trials of the FAT were counterbalanced and randomized for each participant.

Participants were instructed to indicate whether they would want to approach or avoid the combination of threat and reward during the offer and decision phase, by means of pulling or pushing a joystick, respectively. Using similar probabilities as in the monetary titration task, approaching the avatar yielded a 40 percent chance of receiving a negative outcome, a 40 percent chance of receiving a positive outcome, and a 20 percent chance of receiving a neutral outcome. Avoiding the avatar led to a neutral outcome with 80 percent chance and resulted in a positive outcome in 10 percent of the cases and in a negative outcome in 10 percent of the cases.

The offer and decision phase was followed by a jittered anticipation window of 5-7 seconds, indicated by the appearance of a white line underneath the monetary reward value on the screen (provided that participants responded in time). Thereupon, the outcome window was shown for one second. To indicate the outcome of the trial, the avatar on the screen would draw a gun and shoot in case of a negative outcome, or would show a pile of banknotes in case of a positive outcome. A neutral outcome was illustrated by the avatar remaining his hand behind its back. In case of a negative outcome, participants were immediately granted the electrical stimulations. The inter-trial interval varied between 6 and 8 seconds. During this interval, participants were presented with a fixation cross in the centre of the screen. In total, participants completed 10 trials of each trial type, resulting in 90 trials in total. All study details can be found in the projects' pre-registration (Hulsman, Klaassen, Roelofs & Klumpers, 2021).

Figure 1

Layout of the FAT

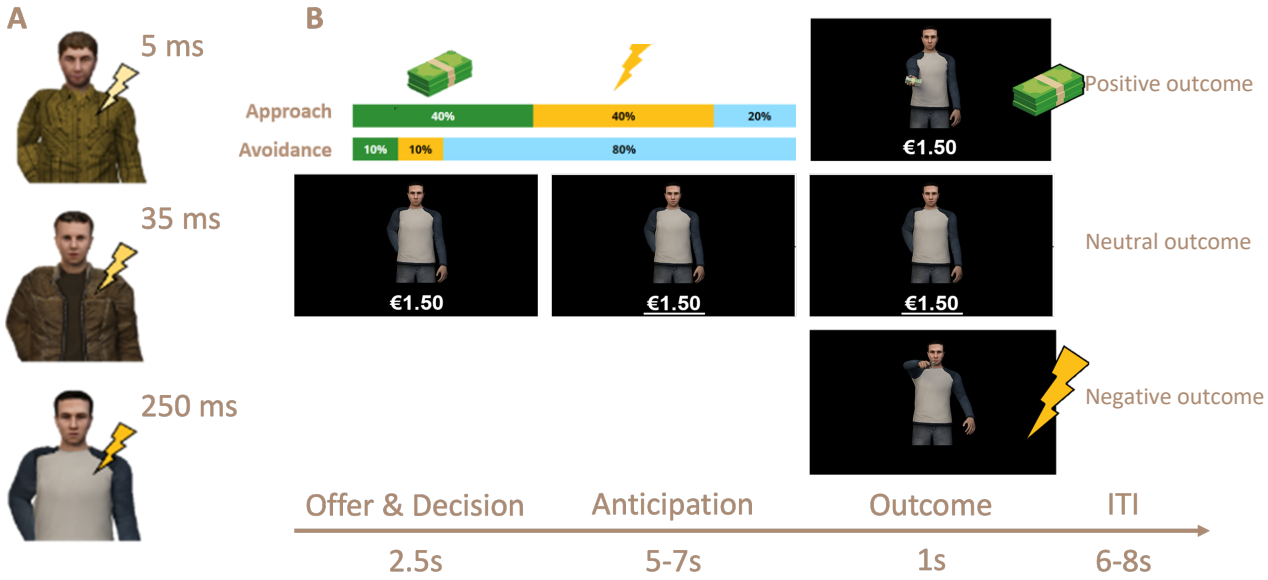

note. This figure includes a visual representation of the outline of the Fearful Avoidance Task (B) and the different avatars, that corresponded to different levels of threat (A). At the start of every trial, the monetary reward would be presented together with one of the three avatars. During the offer & decision phase, participants had to decide to approach or avoid this combination of potential reward and potential threat, by pulling or pushing a joystick, respectively. When the response was made in time, a white line would appear underneath the monetary reward value, indicating the anticipation phase. Upon the anticipation, the outcome was showed on the screen. The probabilities of getting a positive, negative, or neutral outcome depended on the participant's decision, and are indicated at the top of the figure. After the outcome was presented, a fixation cross appeared on the screen during the inter-trial interval (ITI).

Behavioural analysis

The aim of this study was to identify patterns of activity that are related to approach-avoidance decision-making. To be able to distinguish neural patterns that differentiate between approach and avoidance decisions, we first established whether there was sufficient variance in approach and avoidance decisions, by analysing the behavioural avoidance responses. We investigated whether approach-avoidance decision-making varied as a function of reward and threat level. Previous research has shown that threat and reward have opposing effects on the proportion of avoidance responses (Hulsman et al., 2021). We expected to find similar patterns in this experiment.

The variance in approach-avoidance responses as a function of the level of threat and reward was investigated with a Bayesian mixed-effects model, using a Bernoulli distribution to model the binary nature of the responses. We used the response (being either approach or avoid) as the outcome of interest. Predictors in this model were the reward and threat level of the trial, as well as the interaction between the reward and threat, which resulted in three fixed effects for our statistical model. We also added a random intercept to model the repeated measures' nature of the data. No random slopes were added for the reward and threat levels, because the relatively small sample size did not allow for the addition of more random effects, as this would lead to convergence issues as well as model fitting complications. All random correlation terms among the random effects were included. The

grouping variable for the analysis was the participant code. The specific model of our main behavioural analysis was defined as follows:

$$Response \sim Rewardlevel * Threatlevel + (1 \mid Participant\ Code)$$

The model fit was analysed using posterior predictive checks. All analyses were performed using R Studio (v 1.4.1717) and R version 4.1.1 (RStudio Team, 2021; R Core Team, 2020). The mixed-effects models were run with the brm function of the 2.16.1 version of the brms package (Bürkner, 2017) and the emmeans and emmtrends function of the 1.8.0 version of the emmeans package (Lenth, 2022). The figures related to the behavioural data analysis were created with the 3.3.5 version of the ggplot2 package, the 0.20.44 version of the lattice package, and the 3.0.11 version of the car package (Wickham, 2016; Neuwirth, 2022; Deepayan, 2008; Fox & Weisberg, 2019).

MRI data acquisition and processing

The fMRI data were acquired on a 3T MRI system (PrismaFit, Siemens), using a 32-channel head coil. First, a T1-weighted scan of 192 sagittal slices with a 1.0 mm isotropic voxel size was obtained using a 3D MPRAGE sequence (TR = 1500 ms, TE= 3.03 ms, FOV = 256 mm). The functional images were obtained using a 2.5 mm isotropic multiband, multi-echo (MBME) sequence (TR = 1500 ms, $TE_{1\text{-}3}$ = 13.4/34.8/56.2 ms, flip angle = 75°, 51 sagittal slices). Both multiband and multi-echo acquisition techniques are designed to improve the quality of the fMRI data (Kovářová, Gajdoš & Mikl, 2022). Combined multiband multi-echo sequences have been shown to improve the specificity and sensitivity of task-related fMRI data compared to standard multi-echo fMRI sequences and were therefore used for the imaging of this study (Boyacioğlu, Schulz, Koopmans, Barth & Norris, 2015).

The fMRI data were processed and the general linear model analysis was conducted using SPM 12 (Wellcome Trust Centre for Neuroimaging, London, UK). All functional scans were combined and realigned using a PAID weighting (Kundu et al., 2017). Pre-processing entailed co-registration of all functional scans to the anatomical scan and normalization to the Montreal Neurological Institute (MNI) 152 T1-template. The normalized images were then smoothed using a 6 mm full width at half maximum 3D isotropic Gaussian kernel. For each participant, a general linear model analysis was conducted that included 38 regressors. That is, each block of trials was assigned a regressor for the offer phase that was followed by an approach response, the offer phase that was followed by an avoidance response, the anticipation phase after an approach response, the anticipation phase after an avoidance response, the outcome phase for a positive, negative and neutral outcome, the offer phase of a nonresponse, the anticipation phase after a nonresponse, the negative outcome that followed a nonresponse, and a constant. A default high-pass filter cut-off of 128 seconds was used, and the models were estimated using classical Restricted Maximum Likelihood methods.

MVPA

To be able to train and test a classifier, we split up the data into 5 chronological trial blocks, each consisting of 18 consecutive trials. This data was then analysed using a leave one out between-run cross-validation using a spherical searchlight analysis, with a default searchlight diameter of three voxels centred around each voxel in the brain (Peer & Epstein 2021;

Levorsen, Ito, Suzuki & Izuma, 2020; Wake & Izuma, 2017; Suzuki, Cross & O'Doherty, 2017; McNamee, Liljeholm, Zika & O'Doherty, 2015; Jimura & Poldrack, 2012). We specifically kept the searchlight diameter at three voxels, to be able to identify the importance of small brain regions such as the amygdala for the classification, as well as to be more precise in where the classifier-relevant regions were located in the brain. That is, increasing the searchlight size increases the number of false positives in the searchlight map (Etzel, Zacks & Braver, 2013). The searchlight analysis was performed using the template script of The Decoding Toolbox, version 3.999E (Hebart, Görgen & Haynes, 2015), and was performed on the whole brain. The results of the searchlight analysis were tested in SPM 12 (Wellcome Trust Centre for Neuroimaging, London, UK).

For every subject, we performed a separate searchlight analysis. The classification of interest was focussed on the offer phase, during which participants made and indicated their decision to approach or avoid. The classifier was hence trained and tested to identify patterns of neural activity belonging to avoid versus approach trials during the offer phase. The classification accuracy and corresponding whole brain contrast maps were obtained. Subsequently, the single subject accuracy maps gained from the classification were combined into group accuracy maps. Images reflecting the classifier pattern were created using MRIcroGL (https://www.nitrc.org/projects/mricrogl). The overall accuracy per participant of the complete searchlight was compared against chance using an independent samples t-test (Zhat et al., 2022; Filimon, Rieth, Sereno & Cottrell, 2014).

Additionally, to further explore the classification accuracy of different parts of the brain, we extracted the accuracy information from several nuclei in the brain, being the thalamus, ACC, dACC mPFC and mOFC, as these regions have been reported to be associated with decision-making (Mitchell, 2015; Hulsman et al., in prep.; Ironside et al., 2020; Livermore et al., 2021; Bertoux et al., 2014). We furthermore explored the classification accuracies in the NAcc, an important reward-related hub in the brain, and in the amygdala, as this region is commonly associated with fear and threat (Öhman, 2005; Mattavelli et al., 2014; Hulsman et al., in prep.). We also extracted the accuracy information from other regions that resulted from our whole-brain searchlight analysis. To explore how accurate these brain regions were at classifying approach and avoidance decisions, we extracted the mean accuracy that resulted from these regions as a measure of overall accuracy of that particular brain region in decoding approach-avoidance responses. Furthermore, as the additional value of multivariate pattern analysis is to be able to analyse smaller sub-regional patterns, we extracted the peak accuracy per brain region. However, as the different brain regions varied in size and hence in the amount of voxels, we also extracted the 98th percentile accuracy from all voxel accuracies within each region, to correct for false positive single-voxel classificiation accuracies.

Results

Behavioural analyses

The behavioural avoidance responses as a function of reward (figure 2B), threat (2C) and the interaction between reward and threat (figure 2A) are shown in the figure below.

Figure 2

Plots showing the effects of reward and threat on the proportion avoidance responses

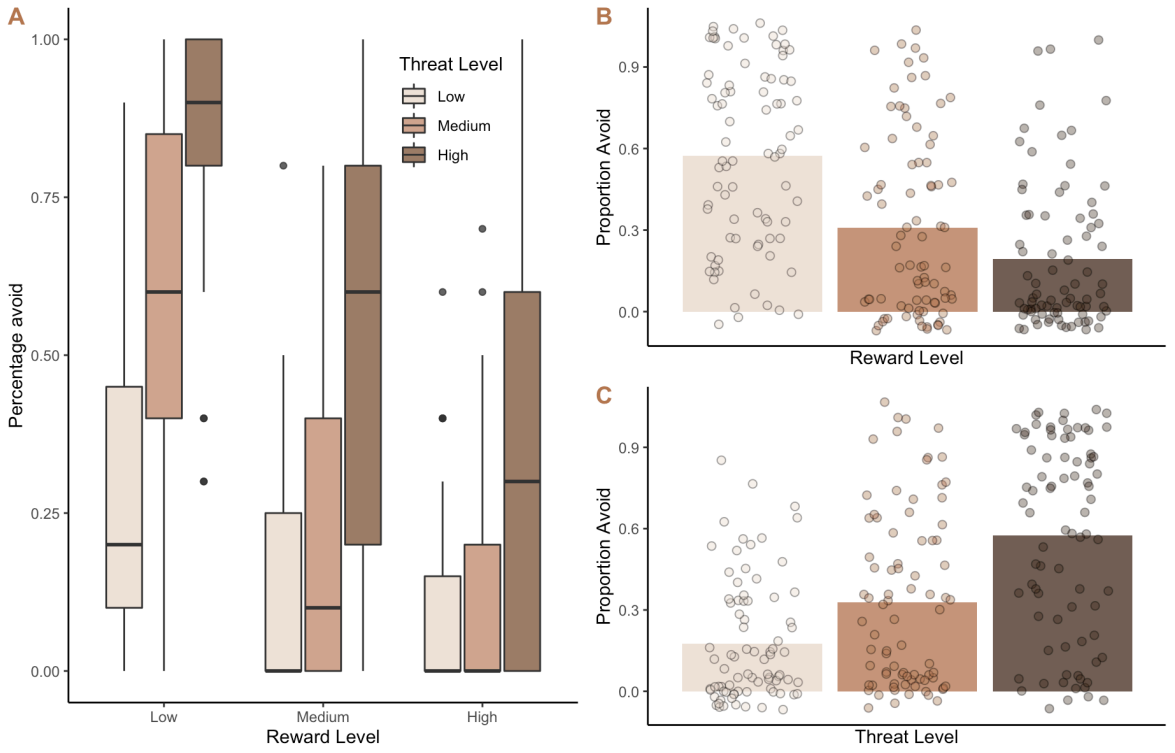

note. This figure shows the interaction between reward and threat on approach-avoidance decision-making (A) as well as the main effect of reward (B) and threat (C) on approach-avoidance decisions in the FAT. The main effects of reward and threat are overlayed with the individual data points to indicate variance between subjects.

The main effect of reward is visualized in figure 2B. The effect was significant between all three levels of reward (Low-Medium reward: *b* = 1,53, 95% CI [1.26, 1.76]; Medium-High reward: *b* = .75, 95% CI [.47, 1.00]; Low-High reward: *b* = 2.28, 95% CI [2.00, 2.57]). Similarly, the effect of threat was significant between all levels of threat (Low-Medium threat: *b* = -.89, 95% CI [-1.16, -.61]; Medium-High threat: *b* = -1.53, 95% CI [-1.79, -1.29]; Low-High threat: *b* = -2.43, 95% CI [-2.69, -2.13]). These opposing effects of reward and threat were also notified by Hulsman and colleagues (2021).

Besides the main effects of threat and reward, there was an interaction between threat and reward on the proportion of avoidance responses. That is, the incline in avoidance responses as a function of threat level is on average much steeper in low reward levels, as compared to medium and high reward levels (see figure 2A and the *b*-values in table 1). All interactions (except from the interaction effect of high reward on low versus medium threat levels) were significant.

Table 1

Estimates and 95% Credible intervals for all threat intervals per reward level

		b	95% CI	
Low reward				
	Low-Medium threat	-1.69	-2.08	-1.29
	Medium-High threat	-1.37	-1.7	-.94
	Low-High threat	-3.06	-3.48	-2.57
Medium reward				
	Low-Medium threat	-.67	-1.16	-.22
	Medium-High threat	-1.78	-2.23	-1.39
	Low-High threat	-2.46	-2.91	-1.98
High reward				
	Low-Medium threat	-.30	-.88	.25
	Medium-High threat	-1.44	-1.89	-.99
	Low-High threat	-1.75	-2.23	-1.25

note. This table shows the estimates and 95% credible intervals for the interaction between reward and threat. That is, the difference between all threat levels is displayed for each level of reward. The effect that was insignificant is marked in grey.

MVPA

The overall classification accuracies of the whole-brain searchlight approach-avoidance decisions were 44.4 and 58.5 percent, respectively. This resulted in an overall classification accuracy of 51.48 percent, which did not differ significantly from chance, $t(26) = .58$, $p = .57$. However, the searchlight analysis revealed several regions and sub-regional clusters in the brain that yielded higher classification accuracies. The most informative regions for the classification between approach and avoidance decisions are shown in figure 3 below, and included the Primary Motor Cortex (M1), the Anterior Cingulate Cortex (ACC) and dorsal ACC (dACC), medial Orbitofrontal Cortex (mOFC) and dorsomedial Prefrontal Cortex (dmPFC).

Figure 3

MVPA Classifier above-chance accuracy map

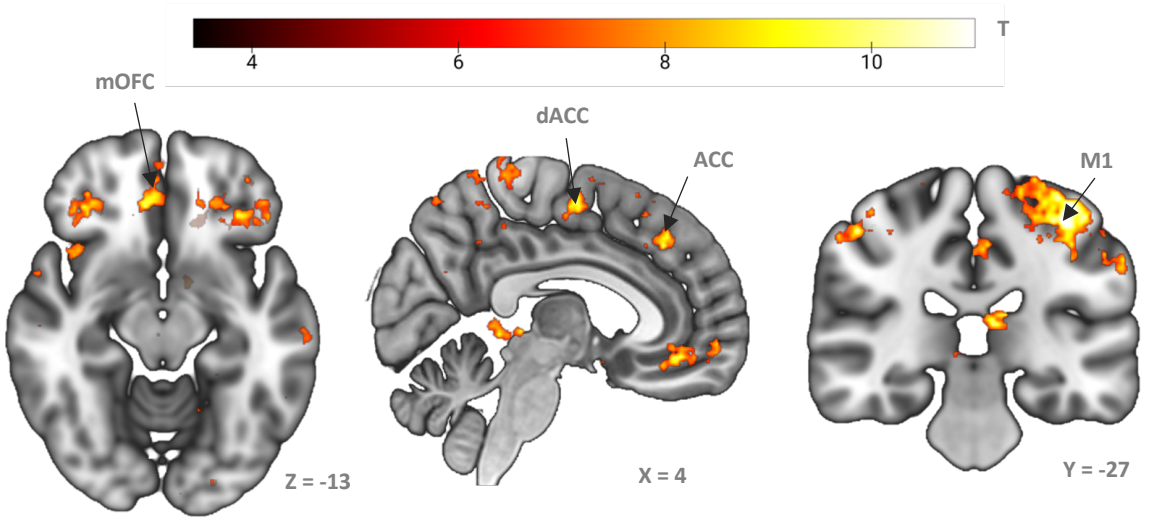

note. This figure shows the brain network that explained significant variation in classifying the patterns of neural activity (reflected by the T-value) of approach-avoidance decision-making during the FAT. The most prominent regions for this classification were the M1, ACC, dACC, mOFC and mPFC. The image is thresholded at an uncorrected *p*-value of .001.

The group-level whole-brain analysis revealed that the motor areas (precentral and postcentral gyrus), as well as the mPFC, mOFC and precuneus significantly predicted the approach-avoidance decisions that were made by the participants (see table 2). To get an overview of all regions that were marked to be of significant importance in the decoding of approach-avoidance decisions, we visually displayed the approach-avoidance network regions in figure 4.

Table 2

Significant brain regions in classifying approach-avoid decisions

	MNI peak coordinates				
Region	x	y	z	Voxels	P (FWE-corr)
Avoid > Approach					
Postcentral gyrus	52	-30	52	27	.02
Precentral gyrus	-38	-26	66	368	< .001
mPFC-left	0	34	40	51	<.001
mPFC-right	36	24	46	69	<.001
mOFC-right	32	38	-14	46	<.001
Precuneus L	-18	-62	54	32	<.001

note. This table shows the MNI peak coordinates, number of voxels and family-wise error corrected *p*-values after an initial voxel-wise threshold of *p* = .001 for brain regions that were of significant importance for approach-avoidance classification.

Figure 4

Visual representation of the avoid-approach network regions

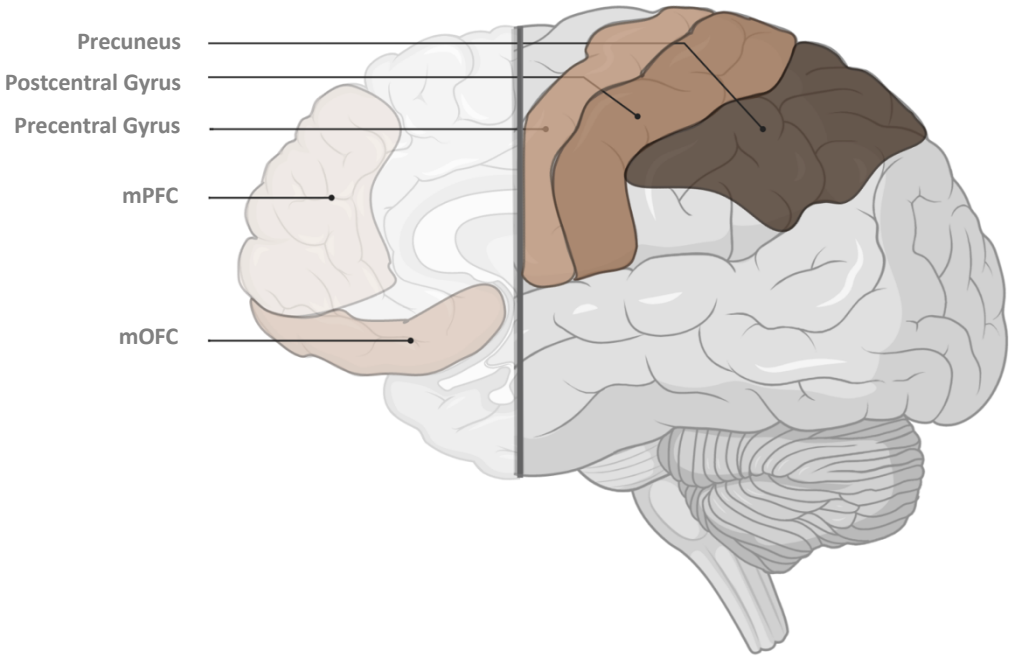

note. This figure displays a visual representation of the brain regions that were important for approach-avoidance decision classification, including the precuneus, pre- and postcentral gyrus, medial prefrontal cortex and medial orbitofrontal cortex.

To further explore how accurate certain (sub-) brain regions were at predicting approach-avoidance responses, we extracted the accuracy information from ten different brain regions (see figure 5). The average accuracy across the different regions as a whole showed varying scores that were all slightly above the chance level of 50 percent across participants, ranging from 51.8 to 53.8 percent accuracy. As a complete region, the lowest performance was reported in the ACC, whilst the highest performance was found in the postcentral gyrus. However, when assessing the peak accuracy within the regions, higher accuracies are reported, varying between 81.5 (NAcc) and 98.5 (postcentral gyrus, precentral gyrus & dACC) percent. To control for the presence of potential false positives, the scores within each region that belonged to the 98th percentile are shown in figure 5C, revealing accuracies ranging from 76.6 (NAcc) to 83.3 (precentral gyrus). Taken all together, besides the regions that resulted from our whole-brain searchlight analysis, it seems that other regions, including for instance the dACC, at least partly consist of voxels that are accurate in predicting approach avoidance behaviour.

Figure 5

Accuracy scores of the classifier in different subregions of the brain

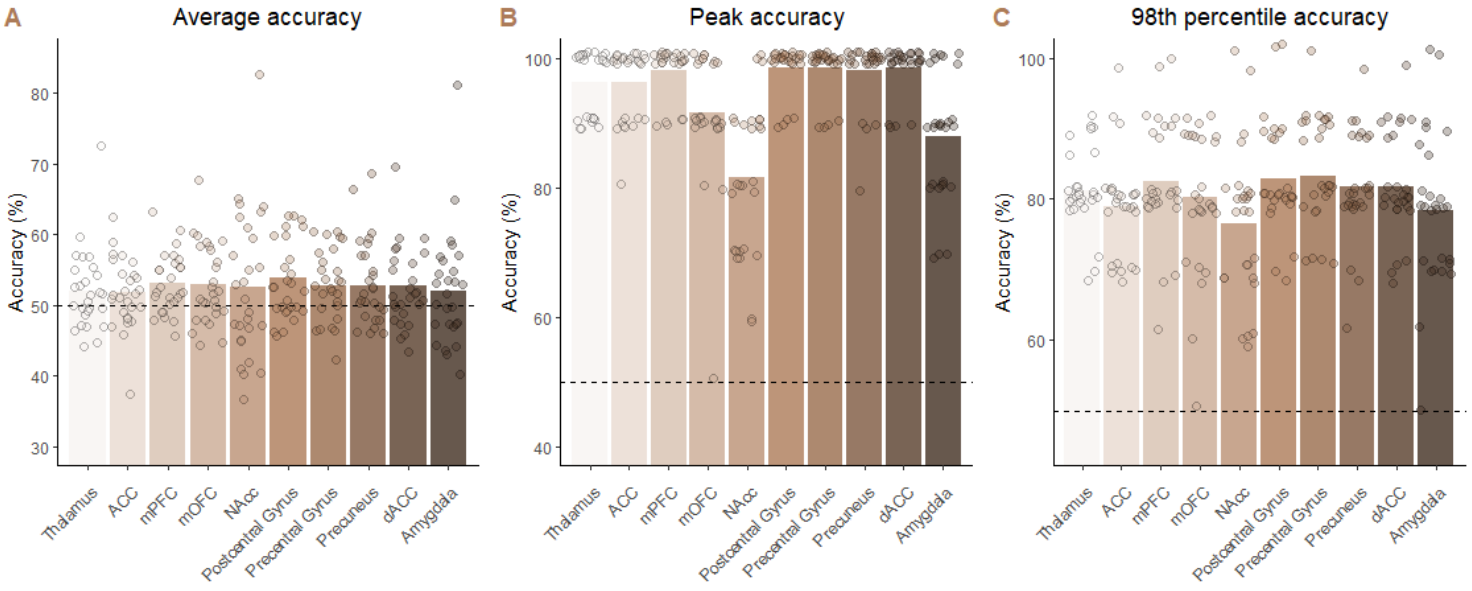

note. This figure shows the mean (A), peak (B) and 98th percentile (C) accuracy scores of the classifier in different (sub-) regions of the brain, during approach-avoidance decision making classification. The average accuracy scores are overlaid with individual data points to indicate variance between subjects. We have chosen to represent the 98th percentile accuracy scores to correct for false positives in larger brain regions. The dashed line represents chance level, being 50 percent.

Experiment 2
Methods

Participants

In total, 15 participants (male = 6, female = 9) were recruited to participate in this study. The mean age of the participants was 28.2 (SD = 11.9 range = 18.9-59.7). This study was part of a larger research project, consisting of multiple measures and tasks. We will only discuss the relevant procedures, materials, and results for the purpose of this thesis.

Participants were compensated for taking part in the study by a fixed monetary reward (€25). Additionally, if the average amount of euros won on two randomly selected trials was above two, participants would receive an additional 5 euros as a bonus. The study was approved by the local ethical committee (CMO region Arnhem – Nijmegen) and was executed in compliance with these guidelines.

Passive-Active Approach-Avoidance Task (PAT)

Preceding the fMRI session with the passive-active approach-avoidance task (PAT), participants took part in a one-hour behavioural session that included the PAT as well. The participants received the instructions for the PAT on the screen, and subsequently practised with the task multiple times. After the behavioural session, the participants were taken to the MRI lab to perform the PAT in the MRI scanner. Participants already underwent a shock-work-up procedure (described in Klumpers et al., 2010) during the behavioural session. However, to titrate the shock level once again for the fMRI session, participants underwent an extra shock-work-up paradigm consisting of three shocks, starting at the same stimulation intensity as the final level from the shock-work-up during their behavioural session. Thereafter, the participant performed 5 practice trials to review their understanding of the task before starting the scanning session. The scanning session consisted of several preparatory scans as well as a resting state scan and a structural scan, before participants would perform the task in the MRI scanner. The task in the MRI scanner consisted of two blocks of 62 trials, lasting about 18 minutes per block.

The PAT (developed by Klaassen et al., 2021) was administered to study people's active and passive decision-making under varying levels of reward and threat. The layout of the PAT is displayed in figure 6 below. A trial always started with a fixation cross, that remained on the screen for the duration of 9-11 seconds. This fixation window was followed by the offer phase, during which the level of threat (indicated by the yellow lightning bolts) and the level of reward (indicated by the green euro signs) of the trial were indicated on the screen. The presentation of this offer phase lasted for 500-7000 ms. During the offer phase, participants were able to think about whether they would want to approach or avoid the combination of reward and threat. Afterwards, the target (the grey circle in the middle) would start moving, either towards the participant (represented by the square on the screen), or away from the participant, for 1000 ms, indicating the response window, during which the participants should put their decision into effect.

Responses were marked as an approach when the target would end up in the same place as the participant, and as an avoid when the target ended up in a different location than the participant. The participant was able to manipulate their position by clicking a button on a button box to jump to the other location (as indicated by the grey bars on the screen) or withhold from clicking the button to stay in the same location.

Trials were considered to be an active approach if the target was moving away from the participant, and the participant pressed the button to approach the combination of reward and threat. Trials were marked as passive approach is the target was moving towards the participant and the participant withheld jumping. An active avoidance trial was characterized by a target that would move towards the participant, and the participant jumping location to

avoid the confrontation with the target. A passive avoidance trial would yield the target to be moving away from the participant, and the participant remaining on the same location.

Similar to the FAT task in study 1, when participants decided to approach, there was a 40 percent chance of receiving a positive outcome (monetary reward), a 40 percent chance of getting a negative outcome (immediate administration of electrical stimulations of 50 ms times the amount of lightning bolts on the screen), and a 20 percent chance of getting a neutral outcome (nothing happens). If the participant chose to avoid the combination of reward and threat, a neutral outcome was guaranteed with 80 percent chance. In 10 percent of the cases, the reward on the screen would be paid out, and in the remaining 10 percent of the cases, participants would receive the electrical stimulations. These probability distributions are shown at the top of figure 6 and resemble the probability distributions of study 1.

When the target had reached its final position, this indicated the end of the response window. To indicate the outcome of the trial, the target's colour would change to green in case of a positive outcome, to yellow in case of the negative outcome, and to light blue in case a neutral outcome was the result of the trial (see figure 6). The outcome window lasted for 1500 ms.

For this task, there were five levels of monetary reward (0 – 4 euros) and five levels of threat (0 – 4 electrical stimulations). The different reward and threat levels were combined in a full-factorial manner, resulting in 25 reward-threat combinations. Per run, each combination of reward and threat was presented twice. In addition, 12 trials with a short offer time window were added to keep the participant engaged and attentive. Taken all together, this resulted in 62 trials per block. All trials were counterbalanced and randomized per participant.

Figure 6

Layout of the PAT

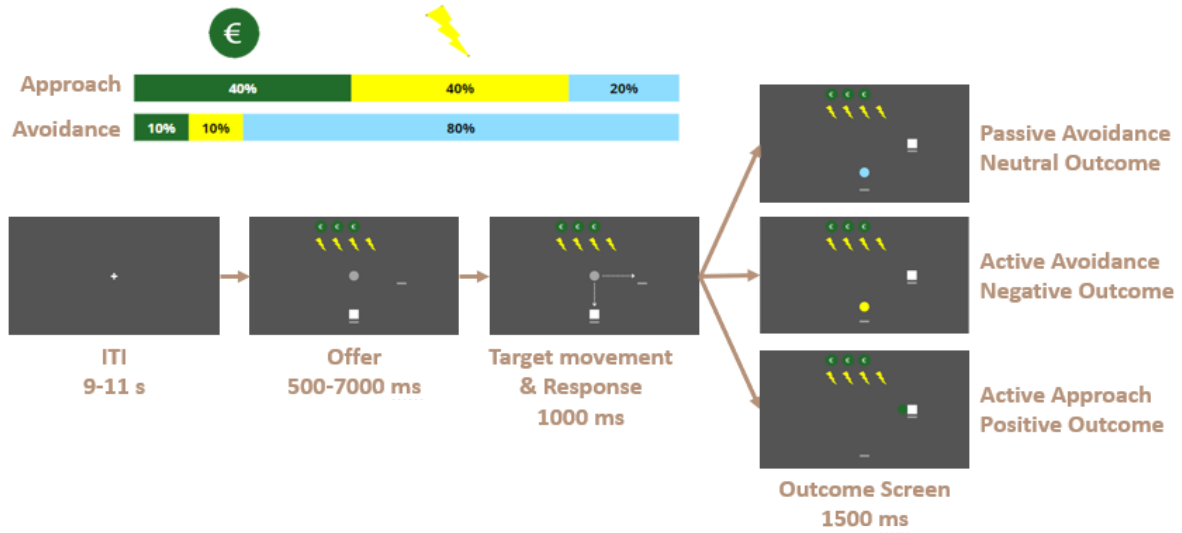

note. This figure shows the layout of the PAT, with the chance distributions of getting either the reward, threat or neutral outcome after an approach or avoidance decision. At the start of every trial, a fixation cross appeared on the screen. Thereupon, the offer phase started, during which the potential reward and threat level of the trial were presented on the screen. During this phase, participants had to decide on whether they wanted to approach or avoid this combination of reward and threat. After the jittered interval had passed, the target (represented by the circle) would start to move

towards or away from the participant (represented by the square), towards one of the two potential end locations (indicated by the two grey bars). When participants wanted to approach the combination of reward and threat, they would have to ensure to end up in the same location as the target after movement, by either withholding from clicking a button (to remain at the start location) or by clicking the button (to jump to the alternative location). If participants chose to avoid the combination of reward and threat, they would have to make sure to not end up in the same location as the target. After the target was done moving, the outcome screen was shown. The target colour would change to light blue (indicative of a neutral outcome), yellow (indicating a negative outcome) or green (indicating a positive outcome). When the outcome was negative, participants immediately received the number of shocks that were on the screen.

Dimensional Anhedonia Rating Scale Questionnaire

The Dimensional Anhedonia Rating Scale (DARS) questionnaire was administered by sending a link to the digital questionnaire to the participants. In this way, participants were able to complete the questionnaire at home, in their own time. The DARS is a dynamic scale that measures peoples' desire, motivation, effort and consummatory pleasure across hedonic domains (Rizvi et al., 2015). The questionnaire consists of 17 items, and has showed to be reliable across studies (Chronbach's α = 0.75-0.92). The different items are rated on a five-point Likert scale from 0 (not at all) to 4 (very much), resulting in a total score between 0 and 68, with higher scores being reflective of less anhedonia.

Behavioural analysis

To investigate whether the PAT elicits an approach-avoidance conflict that results in differential response patterns based on the level of the reward and threat level of the trial, we assessed whether the decision to approach or avoid varied as a function of reward and threat, using a Bayesian mixed effects model that was composed using a Bernoulli distribution to model the binary nature of the responses. The model for this analysis was the same as the one presented in study 1. However, there were now five different levels of reward (0, 1, 2, 3 or 4 euros) and five levels of threat (0, 1, 2, 3, or 4 electrical stimulations). To recapitulate, the model of interest for this analysis was as follows:

$$Response \sim Rewardlevel * Threatlevel + (1 \mid Participant\ Code)$$

Although the combination of 0 reward and 0 threat is not of interest, as performance in these trials contained no information about directed decision-making but was rather performed at random as there was no potential reward nor threat, we chose to include this level in the model for the benefit of the model fit. Based on our findings in study 1 as well as previous literature, we expected a significant main effect of the level of reward, a significant main effect of the level of threat, as well as a significant interaction effect between threat and reward on the proportion of avoidance decisions (Hulsman et al., 2021).

Additionally, as the aim of the second study was to assess the role of anhedonia in approach-avoidance decision-making, we assessed the behavioural variance explained by anhedonia, by adding the centred total scores of the DARS questionnaire to the model. However, due to the limited data available, it was impossible to run the mixed effects model with the interaction between reward, threat, and anhedonia, as the model matrix would be rank deficient and would fail to converge. Therefore, we ran a reduced model that investigated the main effect of anhedonia as well as the effect of the interaction between anhedonia and reward on avoidance decisions, using the following model:

$$Response \sim Rewardlevel * Anhedonia + (1|Participant\ Code)$$

For this model, we again expected a significant effect of reward. Moreover, we expected there to be a significant interaction between anhedonia and reward level. That is, as anhedonia has previously been ascribed to attenuated reward sensitivity, we would expect that participants with higher anhedonia (indicated by lower DARS scores) are less influenced by the reward levels of the trials as compared to people with low anhedonia (Alloy, Olino, Freed & Nusslock, 2016; Liu et al., 2016). All participants completed the DARS questionnaire and were included in these analyses.

Again, the model fit for each model was tested using posterior predictive checks. Just as in our first study, all analyses were performed using R Studio (v 1.4.1717) and R version 4.1.1 (RStudio Team, 2021; R Core Team, 2020). The mixed-effects models were run with the brm function of the 2.16.1 version of the brms package (Bürkner, 2017) and the emmeans and emmtrends function of the 1.8.0 version of the emmeans package (Lenth, 2022). The figures related to the behavioural data analysis were created with the 3.3.5 version of the ggplot2 package, the 0.20.44 version of the lattice package, and the 3.0.11 version of the car package (Wickham, 2016; Neuwirth, 2022; Deepayan, 2008; Fox & Weisberg, 2019).

Results

The results of the behavioural analysis regarding the main effect of reward (figure 7B), the main effect of threat (figure 7C) and the interaction between the reward and threat levels of the trials (figure 7A) on approach-avoidance decision-making, are displayed in figure 7 below.

Figure 7

Plots showing the effects of reward and threat on the proportion avoidance responses

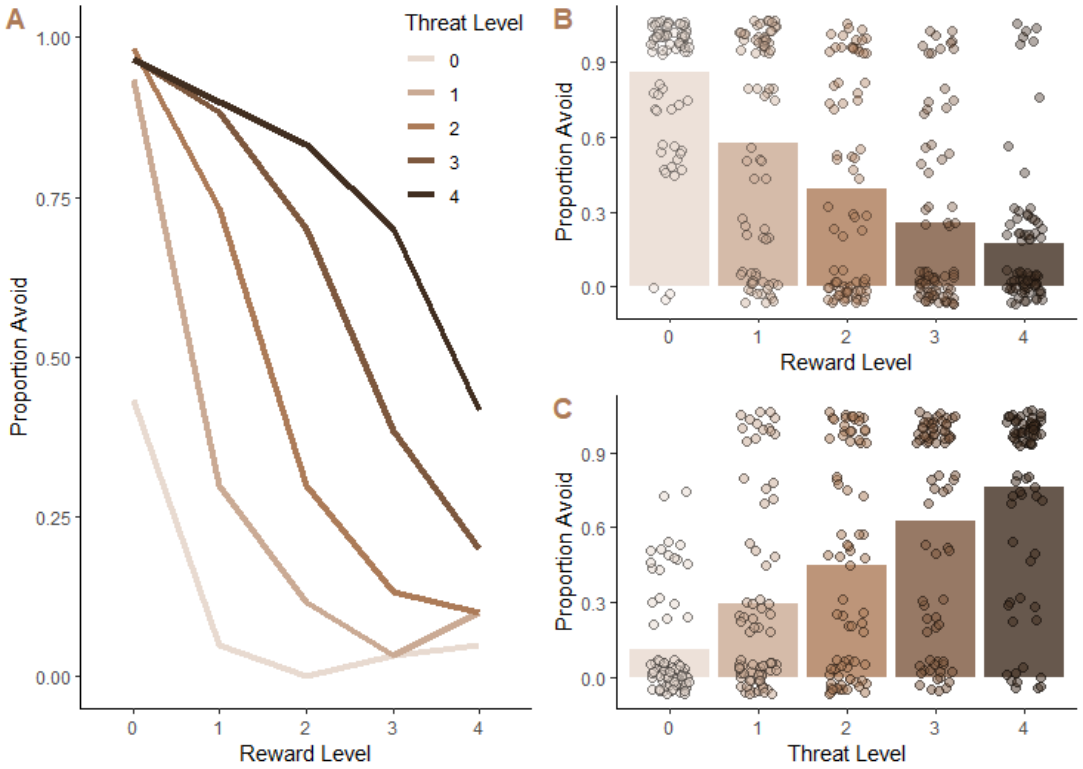

note. This figure shows the interaction between reward and threat on the proportion avoidance decisions (A), as well as the main effect of reward (B) and threat (C) on approach-avoidance decisions in the PAT. The main effects of threat and reward are overlayed with the individual data points to indicate variance between subjects.

The main effect of reward was significant between all reward levels, except from between two and three euros, three and four euros, and two and four euros (see figure 7B and table 3) and showed a decrease in avoidance responses with higher levels of reward. Contrastingly, the number of avoidance responses increased with higher levels of threat. This effect of threat was significant between all levels of threat (see figure 7C and table 3). Furthermore, there was an interaction between threat and reward (figure 7A). This effect of reward on the difference between different levels of threat was significant for almost all interaction terms (see table 3).

Table 3

Estimates and 95% credible intervals for the main- and interaction effects of the PAT

		b	95% CI	
Main effect of reward				
	0-1 euros	3.03	2.26	3.98
	0-2 euros	13.96	3.86	62.43
	0-3 euros	5.52	4.58	6.47
	0-4 euros	5.78	4.91	6.72
	1-2 euros	10.96	0.84	58.95
	1-3 euros	2.48	1.81	3.14
	1-4 euros	2.75	2.18	3.34
	2-3 euros	-8.54	-56.72	1.42
	2-4 euros	-8.28	-56.50	1.69
	3-4 euros	.27	-.38	.91
Main effect of threat				
	0-1 shocks	-11.37	-59.70	-1.35
	0-2 shocks	-12.98	-61.39	-2.71
	0-3 shocks	-14.03	-62.22	-3.90
	0-4 shocks	-14.96	-63.08	-4.50
	1-2 shocks	-1.55	-2.33	-.81
	1-3 shocks	-2.61	-3.27	-1.98
	1-4 shocks	-3.51	-4.21	-2.87
	2-3 shocks	-1.06	-1.76	-.31
	2-4 shocks	-1.97	-2.67	-1.16
	3-4 shocks	-.90	-1.54	-.29
Interaction between threat and reward				
0 euros				
	0-1 shocks	-3.81	-5.15	-2.52
	0-2 shocks	-5.67	-8.61	-3.15
	0-3 shocks	-3.81	-5.15	-2.52
	0-4 shocks	-5.67	-8.61	-3.52
	1-2 shocks	-4.73	-6.53	-3.07
	1-3 shocks	-4.70	-6.80	-3.26
	1-4 shocks	-1.88	-4.84	0.75
	2-3 shocks	-0.92	-2.93	1.09
	2-4 shocks	-0.90	-3.01	1.00
	3-4 shocks	0.94	-1.87	4.18
1 euros				
	0-1 shocks	-2.54	-4.04	-1.18
	0-2 shocks	-5.04	-6.61	-3.71
	0-3 shocks	-6.37	-7.98	-4.80
	0-4 shocks	-6.60	-8.24	-5.02
	1-2 shocks	-2.50	-3.44	-1.60
	1-3 shocks	-3.81	-4.94	-2.73
	1-4 shocks	-4.03	-5.29	-2.93
	2-3 shocks	-1.29	-2.40	-0.14
	2-4 shocks	-1.52	-2.76	-0.46
	3-4 shocks	-0.20	-1.55	1.04
2 euros				
	0-1 shocks	49.70	-290.19	-0.78

	0-2 shocks	-51.16	-292.53	-2.73
	0-3 shocks	-53.42	-294.26	-4.81
	0-4 shocks	-54.20	-295.15	-6.10
	1-2 shocks	-1.47	-2.55	-0.41
	1-3 shocks	-3.74	-4.87	-2.72
	1-4 shocks	-4.75	-5.95	-3.60
	2-3 shocks	-2.28	-3.23	-1.42
	2-4 shocks	-3.28	-4.32	-2.30
	3-4 shocks	-1.00	-2.03	0.03
3 euros				
	0-1 shocks	0.01	-2.35	2.22
	0-2 shocks	-1.79	-3.73	-0.12
	0-3 shocks	-3.52	-5.32	-1.89
	0-4 shocks	-5.40	-7.26	-3.80
	1-2 shocks	-1.78	-3.62	-0.11
	1-3 shocks	-3.54	-5.30	-1.95
	1-4 shocks	-5.41	-7.24	-3.89
	2-3 shocks	-1.75	-2.80	-0.76
	2-4 shocks	-3.60	-4.69	-2.55
	3-4 shocks	-1.87	-2.78	-0.96
4 euros				
	0-1 shocks	-0.86	-2.60	0.62
	0-2 shocks	-0.88	-2.42	0.71
	0-3 shocks	-1.83	-3.47	-0.54
	0-4 shocks	-3.22	-4.72	-1.85
	1-2 shocks	0.00	-1.39	1.24
	1-3 shocks	-0.98	-2.15	0.21
	1-4 shocks	-2.34	-3.51	-1.28
	2-3 shocks	-0.98	-2.15	0.16
	2-4 shocks	-2.34	-3.45	-1.27
	3-4 shocks	-1.38	-2.29	-0.45

note. This table shows the estimates and 95% credible intervals for the main effect of the threat levels, reward levels, and the interaction between threat and reward levels on the approach-avoidance decisions made in the PAT. Insignificant results are marked in grey.

The scores on the Dimensional Anhedonia Rating Scale ranged from 38 to 68 (M = 53.33 SD = 9.90), indicating a relative wide variance in anhedonia scores. That is, the total DARS score usually approximates 57 for control subjects, and 30 for major depressive disorder patients (Rizvi et al., 2015). Analysing our model including the anhedonia scores, we again found that higher levels of reward corresponded to lower levels of avoidance (see table 4). However, we found no evidence for the interaction effect of anhedonia and reward on the number of avoidance decisions (see table 4).

Table 4

Main effects of reward and the interaction effect of reward and anhedonia

		b	95% CI	
Main effect of reward				
	0-1 euros	1.63	1.21	2.04
	0-2 euros	2.46	2.05	2.91
	0-3 euros	3.14	2.68	3.58
	0-4 euros	3.70	3.24	4.17
	1-2 euros	0.83	0.49	1.19
	1-3 euros	1.50	1.15	1.90
	1-4 euros	2.07	1.70	2.49
	2-3 euros	0.67	0.31	1.04
	2-4 euros	1.23	0.85	1.65
	3-4 euros	0.57	0.14	0.98

Interaction between anhedonia and reward			
0-1 euros	0.01	-0.03	0.06
0-2 euros	0.03	-0.01	0.08
0-3 euros	0.03	-0.01	0.08
0-4 euros	0.04	-0.01	0.09
1-2 euros	0.02	-0.02	0.06
1-3 euros	0.02	-0.02	0.05
1-4 euros	0.02	-0.02	0.06
2-3 euros	0.00	-0.04	0.03
2-4 euros	0.01	-0.04	0.05
3-4 euros	0.01	-0.04	0.05

note. This table shows the estimates and 95% credible intervals for the main effect of the reward levels of a trial, and the interaction between anhedonia and reward level of a trial on approach-avoidance decision making in the PAT. Nonsignificant contrasts are marked as grey.

Nonetheless, we did observe a slight nonsignificant negative trend between the proportion of avoidance responses and the anhedonia score, reflecting that people who have higher anhedonia (lower DARS-scores) avoid more than people with lower anhedonia (see figure 8). In addition to these behavioural analyses, we also conducted some preliminary fMRI analyses, which methods and results can be found in the supplementary materials.

Figure 8

Model-based effects plot of anhedonia on the proportion avoidance responses in the PAT

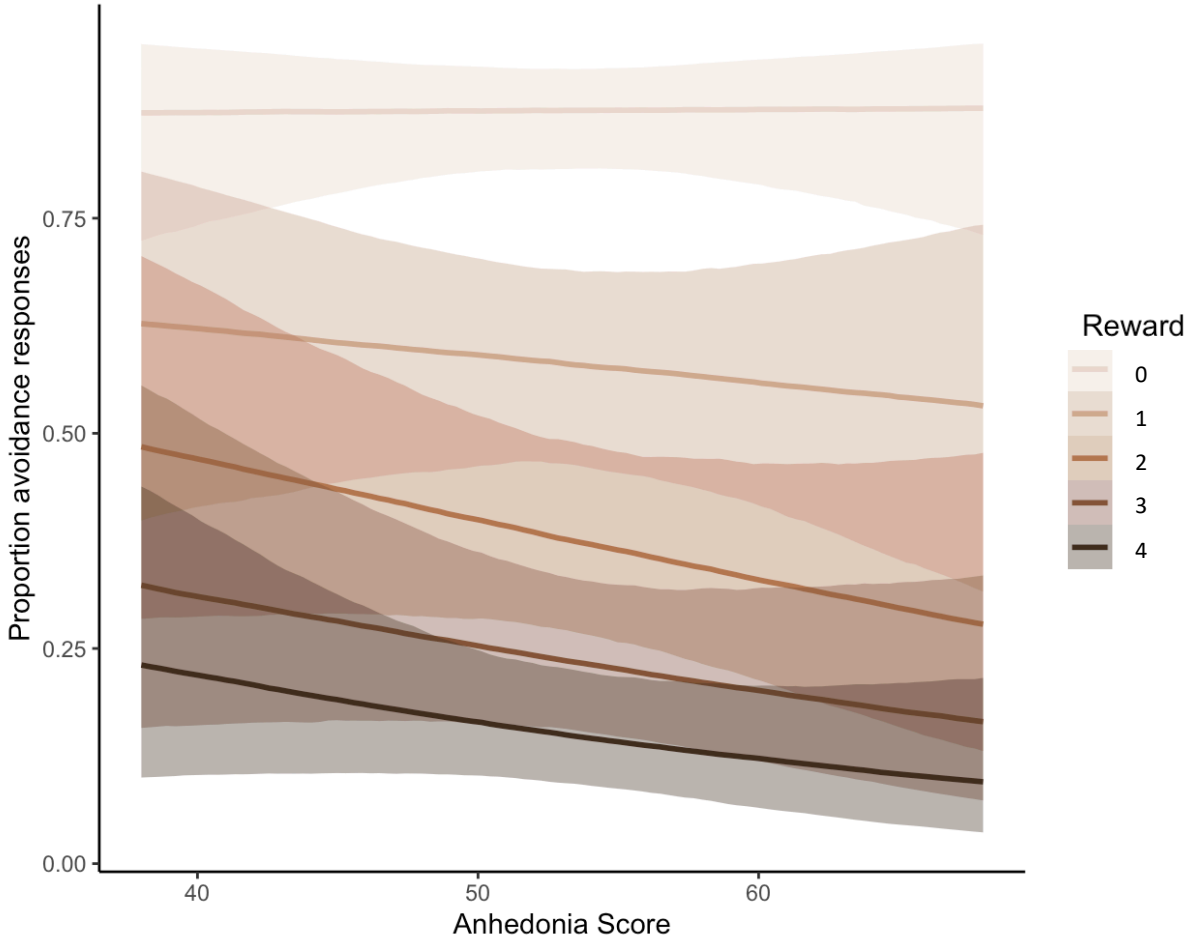

note. This figure shows the model-based effects of the score on the dimensional anhedonia rating scale on the proportion avoidance responses made in the PAT, per level of reward. Higher anhedonia (reflected by lower DARS scores) are associated with more avoidance than lower anhedonia for all reward levels except from reward level 0.

Discussion

In a two-part study, we aimed to deepen our understanding of the behavioural and neural mechanisms of fearful avoidance using two approach-avoidance decision-making tasks. The first part of our study was centred around identifying a network of brain regions involved in approach-avoidance decision-making, using Multi-Voxel Pattern Analysis. We were able to identify a network consisting of six brain regions that performed above chance classification, being the postcentral gyrus, precentral gyrus, bilateral mPFC, the right mOFC and left precuneus. In addition, there were parts of the ACC and dACC that also seemed of importance in classifying the decision to approach or to avoid. In our second study, we explored the effect of anhedonia on approach-avoidance decision-making.

Using a whole-brain searchlight analysis, we revealed bilateral mPFC activity to be explanatory of approach-avoidance decision-making. Research has indicated that increased mPFC activity is related to emotional decision-making (Bertoux et al., 2014; Harris, McClure, van den Bos, Cohen & Fiske, 2007). Additionally, previous research using MVPA methods has too shown that mPFC activity is related to emotional experience (Lieberman, Straccia, Meyer, Du & Tan, 2019), decision impulsivity (Lv, Wang, Chen, Xue & He, 2020), and is also involved in threat anticipation (Qi et al., 2020). With our study, we have therefore confirmed our hypothesis regarding the importance of the mPFC in threat anticipation and emotional decision-making.

Additionally, our classification also revealed that the mOFC could explain approach-avoidance decisions significantly above chance. Although we had no a priori hypothesis for this region to be included in the network, it has been established that the mOFC is important for goal-directed action and that this region also represents reward value (Woon, Sequeira, Barbee & Gourley, 2020; Rolls, Cheng & Feng, 2020). This could explain why the mOFC would be of importance in approach-avoidance decision-making when reward and threat levels are fluctuating.

In addition to these prefrontal regions, we also identified the precentral and postcentral gyrus to be involved in the classification of approach-avoidance decision-making. It could be that these motor regions were included in the network because of the systematic movements that participants were required to make in order to indicate their decision. However, recent research has indicated that motor activity is also required for decision-making itself, rather than just for the initiation of the movement (Zorowitz et al., 2019). With the study design of our first study, we were not able to rule out the motor activity that appeared as a function of movement preparation. However, by adapting the study design in terms of adding passive and active alternatives of both approach and avoid decisions, the design of the second study does allow for the investigation of motor-related activity during decision-making, as the explicit preparation for action related to the specific decision only occurs after the initiation of the target movement. Future research could use paradigms like the PAT to further investigate the role of motor-related brain regions in approach-avoidance decision-making.

Finally, the precuneus was also found to be part of our approach-avoidance decision-making network. Although the precuneus often occurs to be of significance in paradigms focussing on self-processing and consciousness, research has also identified the precuneus to be of

importance in decision-making paradigms (Cavanna & Trimble, 2006; Cavanna, 2007; Garrigan, Adlam & Langdon, 2016; Hall et al., 2021; Paulus et al., 2001). Just as in our results, Paulus and colleagues (2001) found that the precuneus was involved in decision-making in the presence of uncertainty, and suggested that the precuneus has a role in choosing between different choice strategies, as well as keeping track of previous response-outcome occurrences.

Although we did not find evidence for the importance of the amygdala, NAcc, ACC and dACC with our whole-brain analysis, we did find exceptionally high accuracies in parts of the ACC and dACC when we extracted the classification accuracies from these brain regions. This indicates that perhaps smaller, sub-regional clusters of voxels within these regions might be of importance in approach-avoidance decision prediction. Future research should assess if this is the case by for instance using planned ROI-based pattern analyses to assess the importance of these sub-regional clusters in approach-avoidance decision-making.

Now that we have identified that this network is active during avoidance decisions, it would be of interest to investigate its implications in psychopathology. As mentioned, excessive avoidance is a good indication of poor prognosis in psychopathology (Hendriks et al., 2012). It would be interesting to see how activity in this network differs between patients and healthy controls, to see if we can find novel targets for treatment. Research has indicated that the precuneus for instance is connected to brain systems that are implicated in depression, but also in anxiety, as well as predicts symptom severity in people with post-traumatic stress disorder (Cheng et al., 2018; Zhang et al., 2021; Yuan, et al., 2018; Lai, 2018; Geuze, Vermetten, de Kloet & Westenberg, 2007; Rousseau et al., 2019). Moreover, the orbitofrontal cortex has been shown to be implicated in occurrence of depression and anxiety symptoms (Rolls, Cheng & Feng, 2020; Laird et al., 2019). Furthermore, research has shown that altered activity and connectivity in and with the medial prefrontal cortex is seen in many psychopathologies (Hiser & Koenigs, 2018). Future research should investigate whether disruptions in this prefrontal-parietal network can be explanatory of psychopathology, and whether these disruptions can be seen trans diagnostically.

Although the network analysis in study 1 resulted in a promising wide-spread network consisting of brain regions that are involved in decision-making and threat and reward anticipation, we must address some of the limitations of this study. First and foremost, the MVPA analyses were run post-hoc. That is, the study was not set up for the specific purpose of performing MVPA analyses on the resulting data. Therefore, the task design was suboptimal for decoding purposes. More specifically, when one wants to perform classification, one opts for a fully counterbalanced task, preferably with many trials. As the decision to approach or avoid is a voluntary choice, and hence varies between participants, the data were not fully counterbalanced. One way to circumvent this issue is to perform a between-run cross-validation paradigm. However, this specific task only consisted of one run of trials. Therefore, we manually split up the data into five equal blocks of 18 trials, ensuring enough variation in approach-avoidance responses in each block, and ran the classification on the approach versus avoid betas from these different blocks. Even though the design of this task was not particularly set up for classification analyses, we approached the data in such a way that we could reliably run the classification analyses. Additionally, for the scope of this research project, we limited our analyses by only performing a whole brain

searchlight analysis on the approach-avoidance contrast. Knowing that whole brain searchlight analyses bring potential pitfalls, as described by Etzel, Zacks and Braver (2013), it would be interesting to perform follow-up analyses using specific regions of interest to validate the results found in our analyses.

The second part of our study focussed on exploring the effects of anhedonia on excessive avoidance using the passive-active approach-avoidance task. We found that this task elicited similar behavioural responses to the experiment of Hulsman and co-workers (in prep.), in terms of the proportion of avoidance responses based on the different levels of reward and threat. Secondly, we hypothesized that the number of avoidance responses could potentially be influenced by the severity of anhedonia, as a lack of reward sensitivity might bias participants towards more avoidance. In contrast to our hypotheses, we found no evidence that anhedonia interacts with the reward levels of a trial. However, we did find a non-significant trend showing that when anhedonic traits are more prominent, the amount of avoidance is higher. Importantly, due to unforeseen circumstances, the sample of this study was limited, which forces us to interpret these findings with care. Although the model fit of our all models were good, the prediction of the estimates were suboptimal due to the small sample size. Additionally, because of this small sample size, we could not include random slopes for the reward and threat levels, resulting in a more limited model. Finally, as the sample investigated here consisted of healthy controls, the variability in anhedonia scores was confined. In the future, this study will be expanded by means of including more control subjects as well as patients suffering from depression and anxiety disorders. Based on this data, we will be able to draw some well-informed conclusions on whether anhedonia influences approach-avoidance decision-making as well as run maximal model analyses that will outperform the model used in this study in estimating the effects of the different reward and threat levels.

On a neural level, we found some interesting prospects for further investigation. That is, our analyses showed that lower anhedonic traits (indicated by higher anhedonia scores on the DARS questionnaire) may elicit larger neural responses in the inferior parietal lobule. However, as there were some concerns about the quality of the obtained fMRI data, these results should be interpreted with great care. Future studies will result in more well-informed conclusions regarding the neural correlates of approach-avoidance behaviours and the effect of anhedonia, due to the addition of more control subjects and patients. Additionally, future research should explore whether these behavioural and neural correlates can function as targets in the development of novel treatments for these psychopathologies. All preliminary fMRI analyses and results of study 2 can be found in the supplementary materials.

Conclusion

The two presented studies investigated the behavioural and neurological correlates of approach-avoidance decision-making, using two different, yet similar, approach-avoidance paradigms. Both paradigms successfully evoked a reward-threat trade-off conflict, which enables a more complex, ecologically valid investigation of daily-life decision-making. We identified a widespread neural network that was associated with the approach-avoidance decision-making process, including regions involved in emotional experience, decision-making, motor preparation, goal-directed behaviour, and reward and threat assessment.

Furthermore, we found some indications for the importance of anhedonia in explaining individual differences in approach-avoidance decisions. However, due to the small sample size, we should interpret these insignificant findings regarding the effects of anhedonia with care and view them as a promising potential motivation for future research on this topic. Nonetheless, the two studies presented here provide a first step in investigating the correlates of excessive avoidance behaviour seen in depressive and anxiety disorders.

References

Öhman, A. (2005). The role of the amygdala in human fear: Automatic detection of threat. *Psychoneuroendocrinology, 30*(10), 953-958.

Alloy, L. B., Olino, T., Freed, R. D., & Nusslock, R. (2016). Role of Reward Sensitivity and Processing in Major Depressive and Bipolar Spectrum Disorders. *Behavior Therapy, 47*(5), 600-621.

Auerbach, R. P., Alonso, J., Axinn, W. G., Cuijpers, P., Ebert, D. D., Green, J. G., . . . Demyttena. (2016). Mental disorders among college students in the World Health Organization World Mental Health Surveys. *Psychological Medicine, 46*, 2955–2970.

Aupperle, R. L., Melrose, A. J., Francisco, A., Paulus, M. P., & Stein, M. B. (2014). Neural substrates of approach-avoidance conflict decision-making. *Human Brain Mapping, 36*(2), 449-462.

Bürkner, P. C. (2017). brms: An R Package for Bayesian Multilevel Models Using Stan. *Journal of Statistical Software, 80*(1), 1-28.

Basten, U., Biele, G., Heekeren, H. R., & Fiebach, C. J. (2010). How the brain integrates costs and benefits during decision making. *Proceedings of the National Academy of Sciences, 107*(50), 21767-21772.

Bertoux, M., Volle, E., de Souza, L. C., Funkiewiez, A., Dubois, B., & Habert, M. O. (2014). Neural correlates of the mini-SEA (Social cognition and Emotional Assessment) in behavioral variant frontotemporal dementia. *Brain Imaging and Behaviour, 8*, 1-6.

Boyacioğlu, R., Schulz, J., Koopmans, P. J., Barth, M., & Norris, D. G. (2015). Improved sensitivity and specificity for resting state and task fMRI with multiband multi-echo EPI compared to multi-echo EPI at 7 T. *NeuroImage, 119*, 352-361.

Bublatzky, F., Alpers, G. W., & Pittig, A. (2017). From avoidance to approach: The influence of threat-of-shock on reward-based decision making. *Behaviour Research and Therapy, 96*, 47-56.

Carvalho, J. P., & Hopko, D. R. (2011). Behavioral theory of depression: Reinforcement as a mediating variable between avoidance and depression. *Journal of Behavior Therapy and Experimental Psychiatry, 42*(2), 154-162.

Cavanna, A. E. (2007). The Precuneus and Consciousness. *CNS spectrums, 12*(7), 545-552.

Cavanna, A. E., & Trimble, M. R. (2006). The precuneus: a review of its functional anatomy and behavioural correlates. *Brain, 129*, 564-583.

Cheng, W., T, E., Qiu, J., Yang, D., Ruan, H., Wei, D., . . . Feng, J. (2018). Functional Connectivity of the Precuneus in Unmedicated Patients With Depression. *Biological Psychiatry: Cognitive Neuroscience and Neuroimaging, 3*(12), 1040-1049.

Cremers, H. R., Veer, I. M., Spinhoven, P., Rombouts, S. A., & Roelofs, K. (2015). Neural sensitivity to social reward and punishment anticipation in socail anxiety disorder. *Frontiers in Behavioral Neuroscience, 8*.

Cuthbert, B. N., & Insel, T. R. (2013). Toward the future of psychiatric diagnosis: the seven pillars of RDoC. *BMC Medicine, 11*(126).

de Graaf, R., ten Have, M., Tuithof, M., & van Dorsselaer, S. (2013). First-incidence of DSM-IV mood, anxiety and substance use disorders and its determinants: Results from the Netherlands Mental Health Survey and Incidence Study-2. *Journal of Affective Disorders, 149*(1-3), 100-107.

Deepayan, S. (2008). Lattice: Multivariate Data Visualization with R.

Dillon, D. G., Rosso, I. M., Pechtel, P., Killgore, W. D., Rauch, S. L., & Pizzagalli, D. A. (2013). PERIL AND PLEASURE: AN RDOC-INSPIRED EXAMINATION OF THREAT RESPONSES AND REWARD PROCESSING IN ANXIETY AND DEPRESSION. *Depression and Anxiety, 31*(3), 233-249.

Etzel, J. A., Zacks, J. M., & Braver, T. S. (2013). Searchlight analysis: Promise, pitfalls, and potential. *NeuroImage, 78*, 261-269.

Filimon, F., Rieth, C. A., Sereno, M. I., & Cottrell, G. W. (2014). Observed, Executed, and Imagined Action Representations can be Decoded From Ventral and Dorsal Areas. *Cerebral Cortex, 25*(9), 3144-3158.

Fox, J., & Weisberg, S. (2019). An R Companion to Applied Regression (3rd Edition).

Garrigan, B., Adlam, A. L., & Langdon, P. E. (2016). The neural correlates of moral decision-making: A systematic review and meta-analysis of moral evaluations and response decision judgements. *Brain and Cognition, 108*, 88-97.

Geuze, E., Vermetten, E., de Kloet, C. S., & Westenberg, H. G. (2007). Precuneal activity during encoding in veterans with posttraumatic stress disorder. *Progress in Brain Research, 167*, 293-297.

Hall, S. A., Towe, S. L., Nadeem, M. T., Hobkirk, A. L., Hartley, B. W., Li, R., . . . Meade, C. S. (2021). Hypoactivation in the precuneus and posterior cingulate cortex during ambiguous decision making in individuals with HIV. *Journal of NeuroVirology, 27*, 463-475.

Harris, L. T., McClure, S. M., van den Bos, W., Cohen, J. D., & Fiske, S. T. (2007). Regions of the MPFC differentially tuned to social and nonsocial affective evaluation. *Cognitive, Affective, & Behavioral Neuroscience, 7*, 309–316.

Hebart, M. N., Görgen, K., & Haynes, J. D. (2015). The Decoding Toolbox (TDT): A versatile software package for multivariate analyses of functional imaging data. *Frontiers in Neuroinformatics, 8*(88).

Hendriks, S. M., Spijker, J., Licht, C. M., Beekman, A. T., & Penninx, B. W. (2012). Two-year course of anxiety disorders: different across disorders or dimensions? *Acta Psychiatrica Scandinavica, 128*(3), 212-221.

Hiser, J., & Koenigs, M. (2018). The Multifaceted Role of the Ventromedial Prefrontal Cortex in Emotion, Decision Making, Social Cognition, and Psychopathology. *Biological Psychiatry, 83*(8), 638-647.

Hulsman, A. M., Kaldewaaij, R., Hashemi, M. M., Zhang, W., Koch, S. B., Figner, B., . . . Klumpers, F. (2021). Individual differences in costly fearful avoidance and the relation to psychophysiology. *Behaviour Research and Therapy, 137*.

Hulsman, A. M., Klaassen, F. H., Roelofs, K., & Klumpers, F. (2021). *Neural Mechanisms Underlying Fearful Avoidance Behaviour.* Retrieved from www.osf.io/7sm9k

Hulsman, A. M., Klaassen, F. H., Roelofs, K., & Klumpers, F. (in prep.). Reduced activity in the nucleus accumbens predicts subsequent costly fearful avoidance behaivour.

Ironside, M., Amemori, K. I., McGrath, C. L., Pedersen, M. L., Kang, M. S., Amemori, S., . . . Pizzagalli, D. A. (2020). Approach-Avoidance Conflict in Major Depressive Disorder: Congruent Neural Findings in Humans and Nonhuman Primates. *Biological Psychiatry, 87*(5), 399-408.

Jimura, K., & Poldrack, R. A. (2012). Analyses of regional-average activation and multivoxel pattern information tell complementary stories. *Neuropsychologia, 50*(4), 544-552.

Kessler, R. C., Petukhova, M., Sampson, N. A., Zaslavsky, A. M., & Wittchen, H. U. (2012). Twelve-month and lifetime prevalence and lifetime morbid risk of anxiety and mood disorders in the United States. *International Journal of Methods in Psychiatric Research, 21*, 169-184.

Khalid, A., Qadir, F., Chan, S. W., & Schwannauer, M. (2019). Adolescents' mental health and well-being in developing countries: a cross-sectional survey from Pakistan. *Journal of Mental Health, 4*, 389-396.

Klaassen, F. H., Held, L., Figner, B., O'Reilly, J. X., Klumpers, F., de Voogd, L. D., & Roelofs, K. (2021). Defensive freezing and its relation to approach–avoidance decision-making under threat. *Scientific Reports, 11*(12030).

Klumpers, F., Raemaekers, M. A., Ruigrok, A. N., Hermans, E. J., Kenemans, J. L., & Baas, J. M. (2010). Prefrontal Mechanisms of Fear Reduction After Threat Offset. *Biological Psychiatry, 68*(11), 1031-1038.

Kovářová, A., Gajdoš, M., & Mikl, M. (2022). Contribution of the multi-echo approach in accelerated functional magnetic resonance imaging multiband acquisition. *Human Brain Mapping, 43*(3), 955– 973.

Krypotos, A. M., Vervliet, B., & Engelhard, I. M. (2018). The validity of human avoidance paradigms. *Behaviour Research and Therapy, 111*, 99-105.

Kundu, P., Voon, V., Balchandani, P., Lombardo , M. V., Poser, B. A., & Bandettini, P. A. (2017). Multi-echo fMRI: A review of applications in fMRI denoising and analysis of BOLD signals. *NeuroImage, 154*, 59-80.

Lai, C. H. (2018). The regional homogeneity of cingulate-precuneus regions: The putative biomarker for depression and anxiety. *Journal of Affective Disorders, 229*, 171-176.

Laird, K. T., Siddarth, P., Krause-Sorio, B., Kilpatrick, L., Milillo, M., Aguilar, Y., . . . Lavretsky, H. (2019). Anxiety symptoms are associated with smaller insular and orbitofrontal cortex volumes in late-life depression. *Journal of Affective Disorders, 256*, 282-287.

Lamers, F., Van Oppen, P., Comijs, H. C., Smit, J. H., Spinhoven, P., Van Balkom, A. J., . . . Penninx, B. W. (2011). Comorbidity Patterns of Anxiety and Depressive Disorders in a Large Cohort Study. *The Journal of Clinical Psychiatry, 72*(3), 341-348.

Lenth, R. V. (2022). *emmeans: Estimated Marginal Means, aka Least-Squares Means*.

Levorsen, M., Ito, A., Suzuki, S., & Izuma, K. (2020). Testing the reinforcement learning hypothesis of social conformity. *Human Brain Mapping, 42*(5), 1328-1342.

Lieberman, M. D., Straccia, M. A., Meyer, M. L., Du, M., & Tan, K. M. (2019). Social, self, (situational), and affective processes in medial prefrontal cortex (MPFC): Causal, multivariate, and reverse inference evidence. *Neuroscience & Biobehavioral Reviews, 99*, 311-328.

Liu, W. H., Roiser, J. P., Wang, L. Z., Zhu, Y. H., Huang, J., Neumann, D. L., . . . Chan, R. C. (2016). Anhedonia is associated with blunted reward sensitivity in first-degree relatives of patients with major depression. *Journal of Affective Disorders, 190*, 640-648.

Livermore, J., Klaassen, F. H., Bramson, B., Hulsman, A. M., Meijer, S. W., Held, L., . . . Roelofs, K. (2021). Approach-Avoidance Decisions Under Threat: The Role of Autonomic Psychophysiological States. *Frontiers in Neuroscience, 15*.

Lv, C., Wnag, Q., Chen, C., Xue, G., & He, Q. (2020). Activation patterns of the dorsal medial prefrontal cortex and frontal pole predict individual differences in decision impulsivity. *Brain Imaging and Behavior, 15*, 421-429.

Mahmoudi, A., Takerkart, S., Regragui, F., Boussaoud, D., & Brovelli, A. (2012). Multivoxel Pattern Analysis for fMRI Data: A Review . *Computational and Mathematical Methods in Medicine*.

Maldjian, J. A., Laurienti, P. J., Kraft, R. A., & Burdette, J. H. (2003). An automated method for neuroanatomic and cytoarchitectonic atlas-based interrogation of fMRI data sets. *NeuroImage, 19*, 1233-1239.

Mattavelli, G., Sormaz, M., Flack, T., Asghar, A. U., Fan, S., Frey, J., . . . Andrews, T. J. (2014). Neural responses to facial expressions support the role of the amygdala in processing threat. *Social Cognitive and Affective Neuroscience, 9*(11), 1684-1689.

McDermott, T. J., Kirlic, N., Akeman, E., Touthang, J., Clausen, A. N., Kuplicki, R., & Aupperle, R. L. (2021). Test–retest reliability of approach-avoidance conflict decision-making during functional magnetic resonance imaging in healthy adults. *Human Brain Mapping, 42*(8), 2347-2361.

McNamee, D., Liljeholm, M., Zika, O., & O'Doherty, J. P. (2015). Characterizing the Associative Content of Brain Structures Involved in Habitual and Goal-Directed Actions in Humans: A Multivariate fMRI Study. *Journal of Neuroscience, 35*(9), 3764-3771.

Mitchell, A. S. (2015). The mediodorsal thalamus as a higher order thalamic relay nucleus important for learning and decision-making. *Neuroscience & Biobehavioral Reviews, 54*, 76-88.

O'Neil, E. B., Newsome, R. N., Li, I. H., Thavabalasingam, S., Ito, R., & Lee, A. C. (2015). Examining the Role of the Human Hippicampus in Approach-Avoidance Decision Making Using a Novel Conflict Paradigm and Multivariate Functional Magnetic Resonance Imaging. *The Journal of Neuroscience, 35*(45), 15039-15049.

Paulus, M. P., Hozack, N., Zauscher, B., McDowell, J. E., Frank, L., Brown, G. G., & Braff, D. L. (2001). Prefrontal, Parietal, and Temporal Cortex Networks Underlie Decision-Making in the Presence of Uncertainty. *NeuroImage, 13*, 91-100.

Peer, M., & Epstein, R. A. (2021). The human brain uses spatial schemas to represent segmented environments. *Current Biology, 31*(21), 4677-4688.

Pelizza, L., & Ferrari, A. (2009). Anhedonia in schizophrenia and major depression: state or trait? *Annals of General Psychiatry, 8*(22).

Pittig, A., & Scherbaum, S. (2020). Costly avoidance in anxious individuals: Elevated threat avoidance in anxious individuals under high, but not low competing rewards. *Journal of Behavior Therapy and Experimental Psychiatry, 66*.

Pittig, A., Alpers, G. W., Niles, A. N., & Craske , M. G. (2015). Avoidant decision-making in social anxiety disorder: A laboratory task linked to in vivo anxiety and treatment outcome. *Behaviour Research and Therapy, 73*, 96-103.

Pittig, A., Treanor, M., LeBeau, R. T., & Craske, M. G. (2018). The role of associative fear and avoidance learning in anxiety disorders: Gaps and directions for future research. *Neuroscience & Biobehavioral Reviews, 88*, 117-140.

Qi, S., Cross, L., Wise, T., Sui, X., O'Doherty, J., & Mobbs, D. (2020). The Role of the Medial Prefrontal Cortex in Spatial Margin of Safety Calculations . *BioRxiv*.

Richards, J. M., Plate, R. C., & Ernst, M. (2013). A systematic review of fMRI reward paradigms used in studies of adolescents vs. adults: The impact of task design and implications for understanding neurodevelopment. *Neuroscience & Biobehavioral Reviews, 37*(5), 976-991.

Rizvi, S. J., Quilty, L. C., Sproule, B. A., Cyriac, A., Bagby, R. M., & Kennedy, S. H. (2015). Development and validation of the Dimensional Anhedonia Rating Scale (DARS) in a community sample and individuals with major depression. *Psychiatry Research, 229*(1-2), 109-119.

Rolls, E. T., Cheng, W., & Feng, J. (2020). The orbitofrontal cortex: reward, emotion and depression. *Brain Communications, 2*(2).

Rousseau, P. F., Malbos, E., Verger, A., Nicolas, F., Lancon, C., Khalfa, S., & Guedj, E. (2019). Increase of precuneus metabolism correlates with reduction of PTSD symptoms after EMDR therapy in military veterans: an 18F-FDG PET study during virtual reality exposure to war. *European Journal of Nuclear Medicine and Molecular Imaging, 46*, 1817-1821.

Santomauro, D. F., Mantilla Herrera, A. M., Shadid, J., Zheng, P., Ashbaugh, C., Pigott, D. M., . . . Cogen, R. M. (2021). Global prevalence and burden of depressive and anxiety disorders in 204 countries and territories in 2020 due to the COVID-19 pandemic. *The Lancet, 398*(10312), 1700-1712.

Schlund, M. W., & Dymond, S. (2016). The tipping point: Value differences and parallel dorsal–ventral frontal circuits gating human approach–avoidance behavior. *NeuroImage, 136*, 94-105.

Sharma, A. W. (2017). Common Dimensional Reward Deficits Across Mood and Psychotic Disorders: A Connectome-Wide Association Study. *American Journal of Psychiatry, 174*(7), 657–666.

Spielberg, J. M., Miller, G. A., Warren, S. L., Engels, A. S., Crocker, L. D., Banich, M. T., . . . Heller, W. (2012). A brain network instantiating approach and avoidance motivation. *Psychophysiology, 49*(9), 1200-1214.

Suzuki, S., Cross, L., & O'Doherty, J. P. (2017). Elucidating the underlying components of food valuation in the human orbitofrontal cortex. *Nature Neuroscience, 20*, 1780-1786.

Talmi, D., Dayan, P., Kiebel, S. J., Frith, C. D., & Dolan, R. J. (2009). How Humans Integrate the Prospects of Pain and Reward during Choice. *Journal of Neuroscience, 29*(46), 14617-14626.

Trew, J. L. (n.d.). Exploring the roles of approach and avoidance in depression: An integrative model. *Clinical Psychology Review, 31*(7), 1156–1168.

Wake, S. J., & Izuma, K. (2017). A common neural code for social and monetary rewards in the human striatum. *Social Cognitive and Affective Neuroscience, 12*(10), 1558-1564.

Wickham, h. (2016). Ggplot2: Elegant Graphics for Data Analysis.

Woon, E. P., Sequeira, M. K., Barbee, B. R., & Gourley, S. L. (2020). Involvement of the rodent prelimbic and medial orbitofrontal cortices in goal-directed action: A brief review. *Journal of Neuroscience Research, 98*(6), 1020-1030.

Yuan, C., Zhu, H., Ren, Z., Yuan, Z., Gao, M., Zhang, Y., . . . Zhang, W. (2018). Precuneus-related regional and network functional deficits in social anxiety disorder: A resting-state functional MRI study. *Comprehensive Psychiatry, 82*, 22-29.

Zha, R., Li, P., Liu, Y., Alarefi, A., Zhang, X., & Li, J. (2022). The orbitofrontal cortex represents advantageous choice in the Iowa gambling task. *Human Brain Mapping, 43*(12), 3840-3856.

Zhang, B. L. (2015). Mapping anhedonia-specific dysfunction in a transdiagnostic approach: an ALE meta-analysis. *Brain Imaging and Behavior, 10*(3), 920–939.

Zhang, B., Qi, S., Liu, S., Liu, X., Wei, X., & Ming, D. (2021). Altered spontaneous neural activity in the precuneus, middle and superior frontal gyri, and hippocampus in college students with subclinical depression. *BMC Psychiatry, 21*(1), 1-10.

Zorowitz, S., Rockhill, A. P., Ellard, K. K., Link, K. E., Herrington, T., Pizzagalli, D. A., . . . Dougherty, D. D. (2019). The Neural Basis of Approach-Avoidance Conflict: A Model Based Analysis. *eNEuro, 6*(4).

Supplementary Materials: Preliminary fMRI analyses study 2

Methods

MRI data acquisition and processing

The fMRI data were acquired on a 3T MRI system (Skyra, Siemens), using a 32-channel head coil. A T1-weighted scan of 192 sagittal slices with a 1.0 mm isotropic voxel size was obtained, using a 3D MPRAGE sequence (TR = 2300 ms, TE = 3.03 ms, FOV = 256 mm). The functional images during task performance were obtained using a 2.5 mm isotropic multi-band, multi-echo sequence (TR = 1500 ms, TE_{1-3} = 12.4/34.3/56.2 ms, flip angle = 75°, 51 slices).

Similar to study 1, the FMRI data were processed and analysed using SPM 12 (Wellcome Trust Centre for Neuroimaging, London, UK). All functional scans were combined using a PAID weighting. The scans were co-registered to the anatomical scans and normalized to the Montreal Neurological Institute (MNI) 152 T1-template, just as in study 1. The normalized images were smoothed using a 6 mm full width at half maximum 3D isotropic Gaussian kernel.

For each participant, a general linear model was constructed that included per run the following 13 regressors: offer phase of short trials, offer phase of trials that were followed by an approach decision, offer phase of trials that were followed by an avoidance decision, the response of the stimulus after a short offer phase, approach response, avoidance response, and three regressors for the positive, negative, and neutral outcomes. Six realignment parameters were added per run to control for subject movement during scanning, as well as a constant. A default high-pass filter cut-off of 128 seconds was used and the models were estimated using classical Restricted Maximum Likelihood methods. For the second-level analysis, a covariate was added consisting of the total DARS score, to investigate the neural mechanisms of anhedonia during approach-avoidance decision-making. One participant had to be excluded from the MRI analyses, as there were significant issues regarding the data quality of the fMRI data of the participant.

fMRI analyses

The fMRI analyses consisted of three parts. First of all, we validated the task by investigating whether the task elicited relevant task effects. To do this, we compared the offer phase (where the participants viewed the stimulus screen) to the baseline activity that was measured during the inter-trial interval. We hypothesized that reward and threat related regions, such as the NAcc, dACC and amygdala would show significant activation due to the effects of the task, based on previous literature (Hulsman et al., in prep.). Therefore, we performed a whole-brain analysis, with an initial uncorrected *p*-value threshold of .005, followed by a region-of-interest analysis focussed on the amygdala, NAcc and dACC.

Second, we validated whether the PAT would elicit similar activity as compared to Hulsman and colleagues (in prep.) when investigating the approach contrast during the anticipation window, and moreover, if these results would add novel information to the results we found in study 1 using a multivariate approach. We therefore hypothesised decreased NAcc activity when making avoidance decisions compared to approach decisions (Hulsman et al., in prep.). To test these hypotheses, we again performed a whole-brain analysis, followed by a specific

region-of-interest analysis including the NAcc, together with some threat-related regions as the amygdala, as well as some higher-order regions as the mPFC and mOFC, which were of importance in the classification network of approach-avoidance decisions in study 1. We added the precuneus, precentral and postcentral gyrus as regions-of interest to see if we could demonstrate their involvement in either approach or avoidance decision making using univariate methods.

Finally, we investigated the role of anhedonia in predicting approach-avoid responses in the passive-active approach-avoidance task. We added anhedonia as a covariate to the second-level MRI model that included the approach and avoidance contrasts during the anticipation window, as this window reflected the decision-making phase of the experiment. We again performed a whole-brain analysis (using an initial voxel-wise threshold of p = .005), as well as a region-of-interest analysis in typical reward regions, being the NAcc and mPFC, and explored the role of the precuneus in explaining variance in approach-avoidance decision-making due to anhedonia (Hulsman et al., in prep.; Schlund & Dymond, 2016). The whole-brain peak coordinates of all significant brain regions were transformed into labels, using the WFU Pickatlas toolbox and Automated Anatomical Labelling (Maldjian, Laurienti, Kraft & Burdette, 2003).

Results

fMRI analyses

Anticipation versus baseline

The whole-brain analysis indicated significant activity in the right parietal superior lobe, as well as in the medial prefrontal cortex (see table S1 and figure S1). Our ROI-analysis revealed one significant region-of-interest, being the dorsal ACC (see table S1).

Table S1

Significant whole-brain and ROI results for BOLD responses associated with anticipation

	MNI peak coordinates				
Region	x	y	z	Voxels	P (FWE-corr)
Anticipation > Baseline					
Whole-brain analysis					
Parietal Superior R	18	-66	58	2925	<.001
mPFC	-32	-6	46	887	.01
ROI-analysis					
dACC	-2	20	38	428	.03

note. This table shows the MNI peak coordinates, number of voxels and family-wise error corrected *p*-values for all brain regions that showed significant BOLD-activity for the anticipation, as compared to baseline.

Figure S1

Whole-brain and ROI results for BOLD responses related to anticipation versus baseline

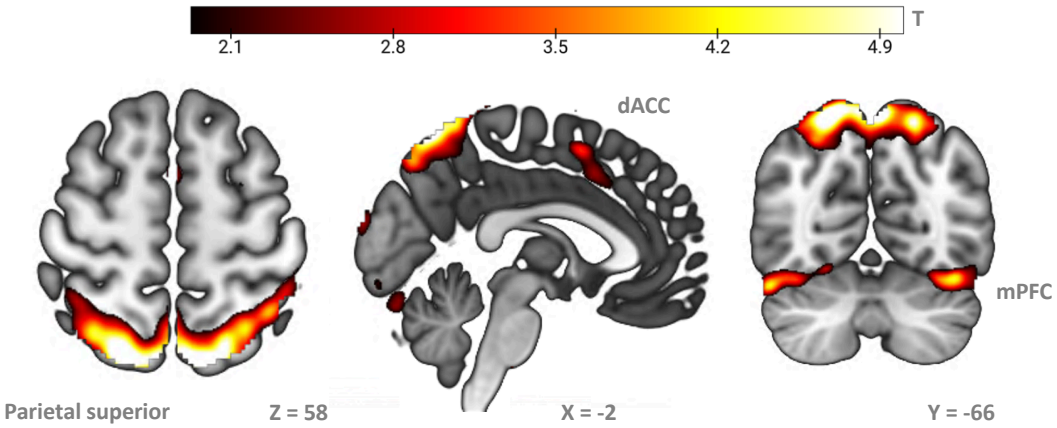

note. This figure shows the whole-brain and ROI effects in the superior parietal lobe, the medial prefrontal cortex, and dorsal anterior cingulate cortex, during the anticipation window of the passive-active approach-avoidance task. An uncorrected *p*-value of .005 was used to create this image.

Approach > avoidance

Our whole-brain analysis revealed no significant clusters to be associated with approach decision making compared to avoidance decision making during the offer phase. Our region-of-interest analysis revealed one marginally significant cluster, being the precentral gyrus (MNI-152: 58, -10, 10, voxels = 30, *p* = .09, see figure S2).

Figure S2

ROI results for BOLD responses related to approach compared to avoidance

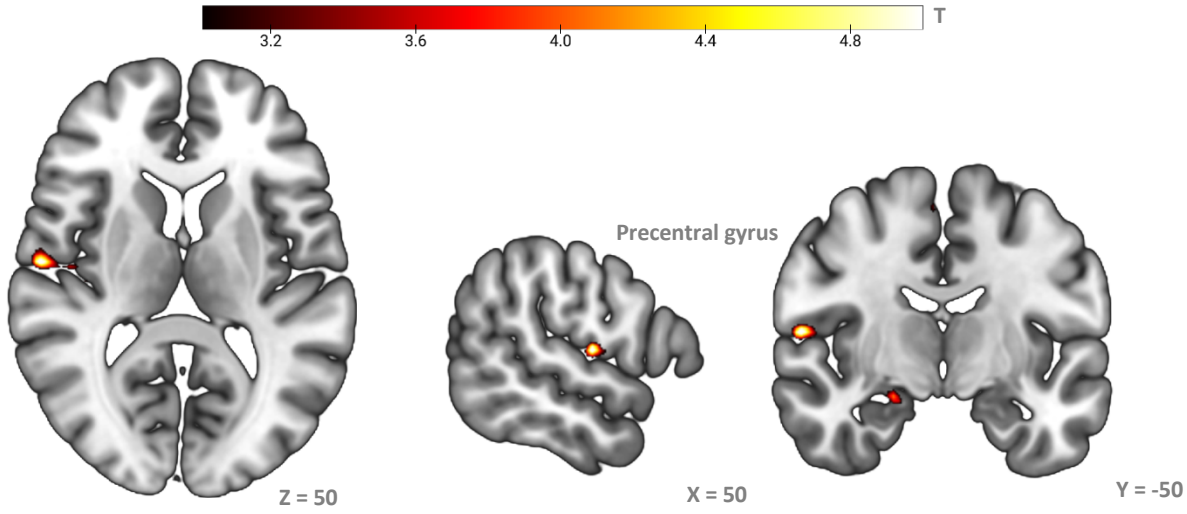

note. This figure shows the ROI effects in the precentral gyrus during the approach decision making in the passive-active approach-avoidance task. An uncorrected *p*-value of .005 was used to create this image.

Avoidance > approach

Our whole-brain analysis identified that, compared to approach decision making, avoidance decisions elicited significant activation in the precuneus (see table S2 and figure S3). Our region-of-interest analysis verified the precuneus as being the only cluster that was significantly involved in avoidance responding. Additionally, the precentral gyrus turned out to be marginally significant.

Table S2

Significant whole-brain and ROI results for BOLD responses related to avoidance compared to approach

	MNI peak coordinates				
Region	x	y	z	Voxels	P (FWE-corr)
Avoid > Approach					
Whole-brain analysis					
Precuneus	20	-64	50	2215	<.001
ROI-analysis					
Precuneus	20	-64	50	762	<.001
Precentral gyrus	58	-10	10	30	.09

note. This table shows the MNI peak coordinates, number of voxels and family-wise error corrected *p*-values for all brain regions that showed significant BOLD-activity for avoidance decisions, as compared to approach decisions.

Figure S3

Whole-brain and ROI results for BOLD responses related to avoidance compared to approach

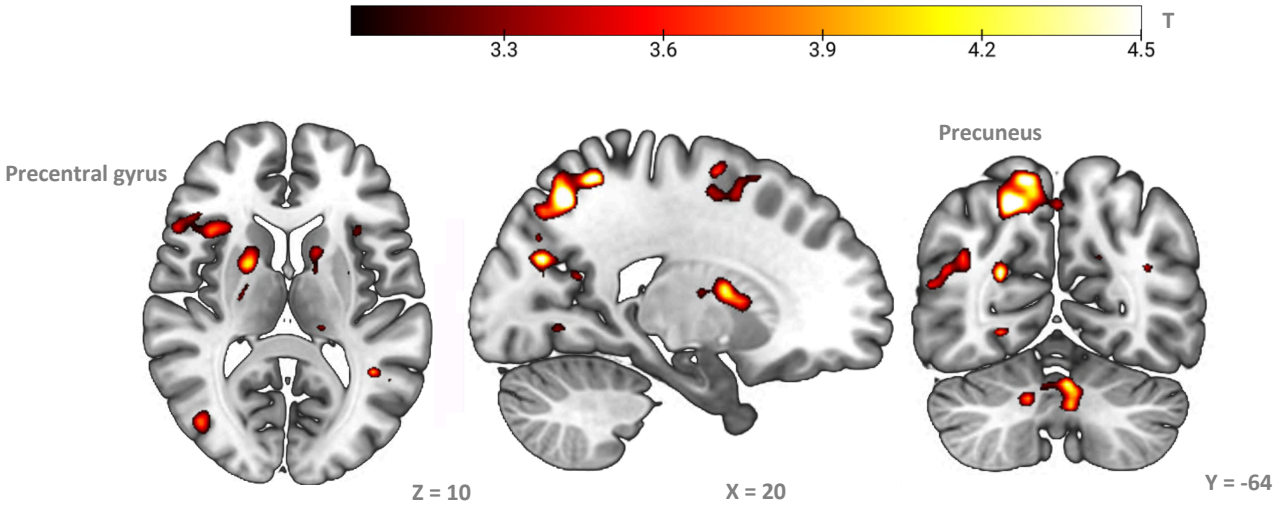

note. This figure shows the whole-brain and ROI effects in the precentral gyrus and precuneus avoidance decision making in the passive-active approach-avoidance task. An uncorrected *p*-value of .005 was used to create this image.

Anhedonia

Our final goal of this study was to investigate the role of anhedonia in approach-avoidance decision making. To this end, we added the scores on the DARS questionnaire as a covariate to the approach-avoidance contrasts. Whole brain analyses revealed a significant positive relationship between activation in the inferior parietal lobule and avoidance decision making (MNI-152: 52, -50, 50, voxels: 1194, p <.001), indicating an increased neural response in the inferior parietal lobule during avoidance decision making in participants with higher anhedonia questionnaire scores (see figure S4). Our region-of-interest analysis did not reveal any significant relationship between anhedonia, the decision to avoid and the NAcc, mPFC or precuneus.

Figure S4

Whole brain results for BOLD responses related to anhedonia during avoidance decisions

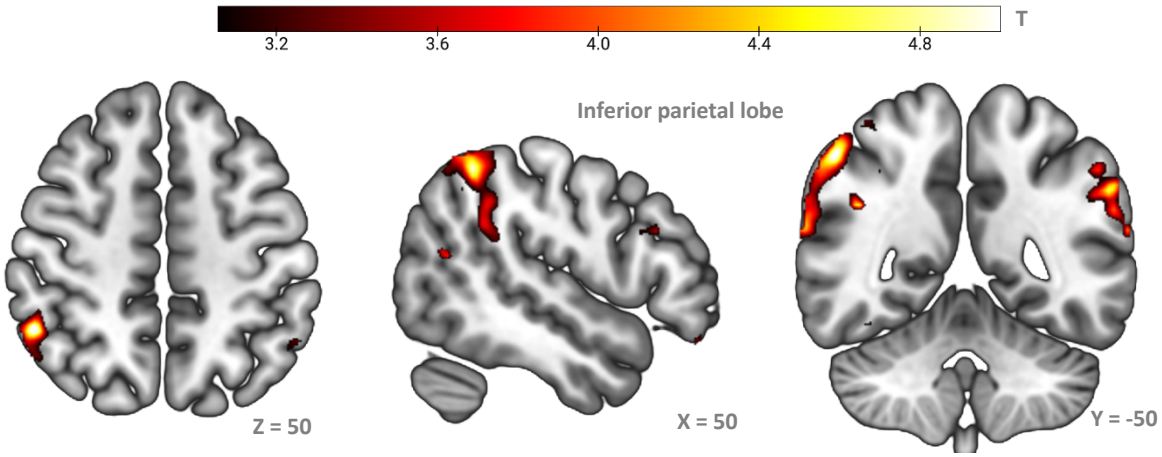

note. This figure shows the whole-brain effects in the inferior parietal lobe as a result of anhedonia during avoidance decision making in the passive-active approach-avoidance task. An uncorrected p-value of .005 was used to create this image.